

### 3. RESULTS AND DISCUSSION

#### 3.1 On-line Size-based Element Speciation for Coal-Mining Disposal Soil Sample in Thailand for the Study of the Release of Heavy Metals into the Environment

On-line size-based element speciation for coal-mining disposal soil sample in Thailand was investigated for the study of the release of heavy metals into the environment.

##### 3.1.1 Coal-mining Overburden Soil Samples

The overburden soil samples consist mainly of larger size particles; 50-75% w/w of the larger size (>1 mm), 20-40% w/w of the medium size (1 mm-0.125 mm) and 3-15% w/w of smaller size (<0.125 mm) (**Figure 3.1**). From the chemical characterisation by XRF, Si and Al are, of course, found as the main elements in the soil (**Figure 3.2**). High amount of S and Fe were found, especially in the LN1 and BP1 samples. The particle size influenced the content of S in the soil. The smaller the particle size, the higher the S content. The high amounts of S and Fe indicate that the soils may contain pyrite ( $\text{FeS}_2$ ) mineral.

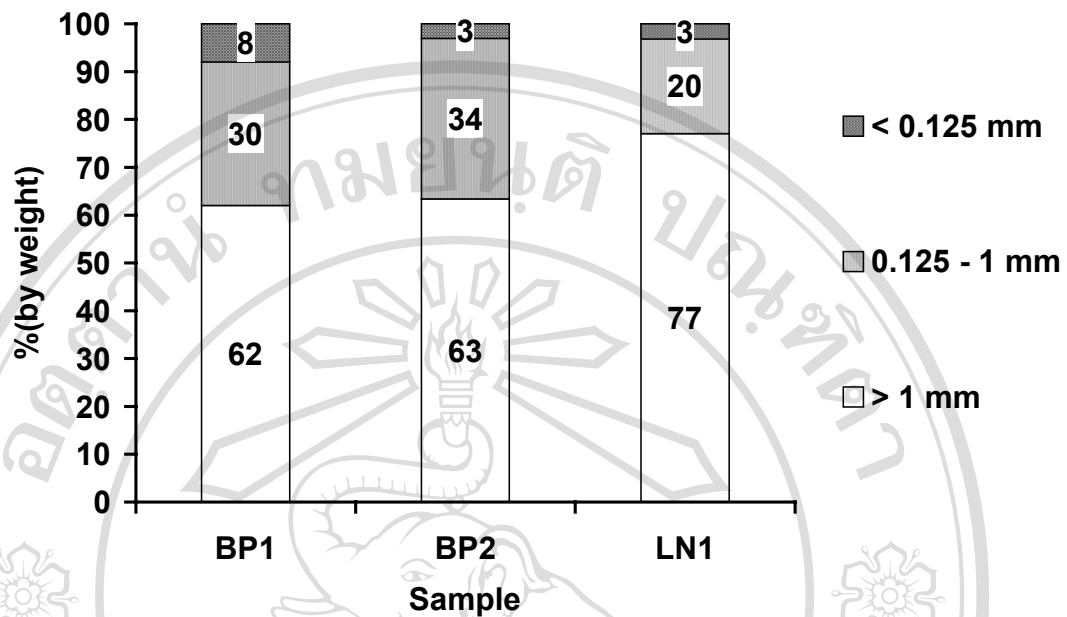
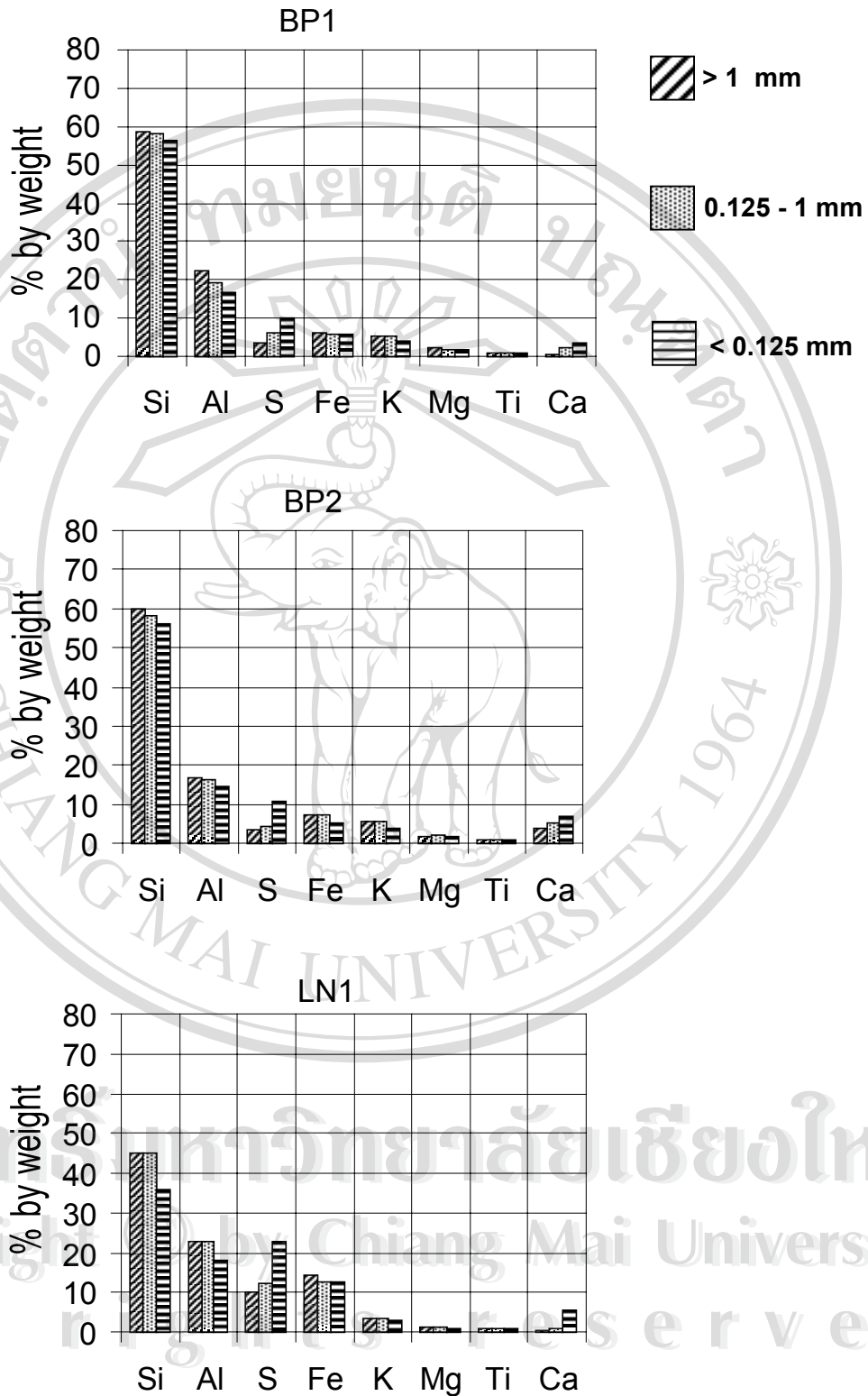


Figure 3.1 Size distribution in the soil samples by sieving



**Figure 3.2** Elemental contents in the different sizes of the soil samples analyzed by

XRF

Pyrite was, therefore, expected to be found in those samples by XRD spectroscopy and SEM. The SEM results showed pyrite and other sulfate mineral phases in those samples (**Table 3.1**) as expected. The XRD diagrams obtained by using the Cu anode did not show any pyrite, but mainly quartz ( $\text{SiO}_2$ ). The XRD with a Mo-anode was therefore performed. The XRD spectrum of the soil sample (**Figure 3.3**) indicated the major phase of quartz and the minor phases of pyrite and the oxidised products of pyrite, jarosite ( $\text{KFe}_3(\text{SO}_4)_2(\text{OH})_6$ ), gypsum ( $\text{CaSO}_4 \cdot 2\text{H}_2\text{O}$ ) and additionally muscovite ( $\text{KA}_1\text{Si}_3\text{O}_{10}(\text{OH})_2$ ) and kaolinite. Whereas, XRD analysis of the BP2 sample (**Figure 3.3**), for which the XRF results show low contents of S and Fe, did not show the peaks of pyrite and jarosite but mainly those of quartz, gypsum and muscovite.

**Table 3.1** SEM results, using back-scattered electron technique

Sample	Mineral found
BP1	$\text{FeS}_2$ , CuS, $\text{CaSO}_4$ , La-phosphate
BP2	$\text{FeS}_2$ , $\text{BaSO}_4$
LN1	$\text{FeS}_2$ , $\text{CaSO}_4$

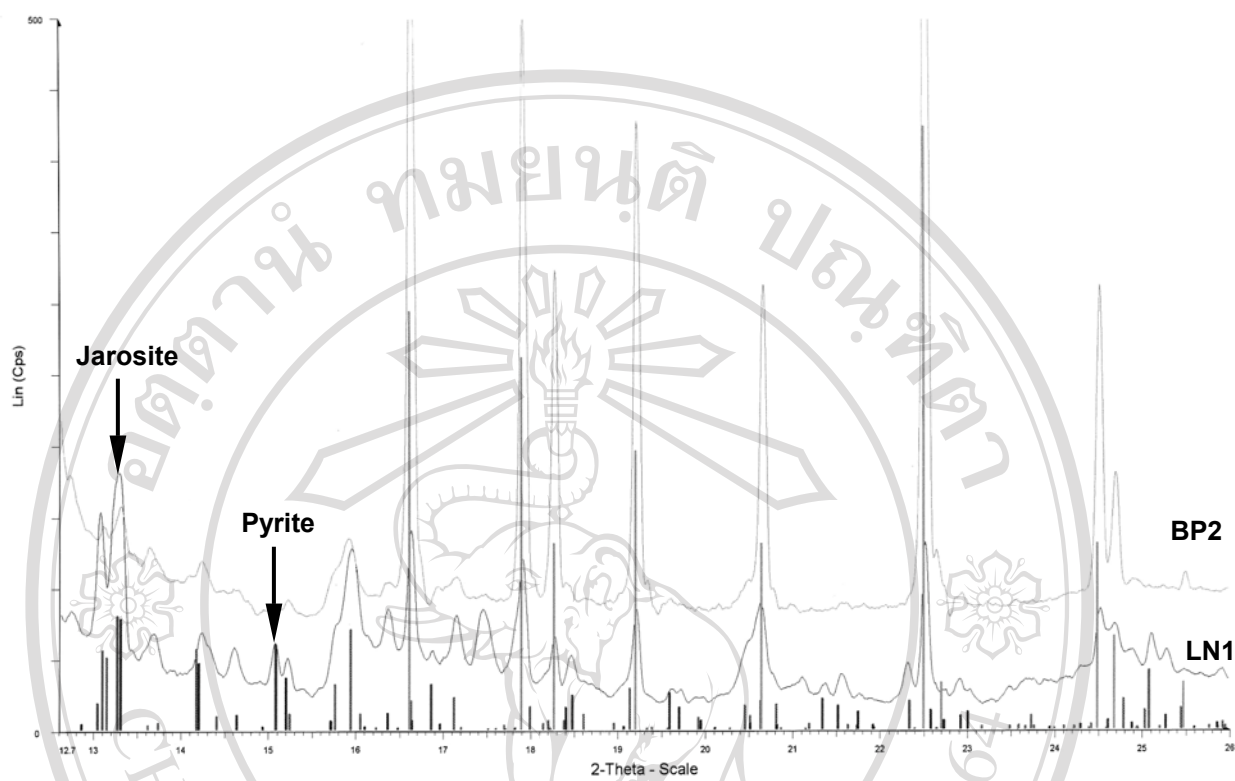


**Figure 3.3** XRD spectra of the BP2 and LN1 samples

The results from ICP-MS analysis of the digested samples (**Table 3.2**) indicated high concentration of Fe, especially in the LN1 sample as found by XRF. There are also other heavy metals existing in the soil samples such as Mn, Ni, Pb, Cd and As partly in a range of  $\mu\text{g/g}$ . Most of carbon matter in the soil sample is organic carbon since the concentration of the inorganic carbon was less than 0.01% wt (**Table 3.2**). The organic carbon contents in LN1 and BP1 samples were relatively high, compared with BP2 samples, likely due to lignite residues in the tailing material.

**Table 3.2** Element concentrations and carbon content in the soil samples (the mixture of the soils of medium and smaller sizes) determined by ICP-MS after digestion using microwave-assisted method

Element*	BP1	BP2	LN-1
<i>Al, mg/g</i>	28.5	55.3	♠
<i>Fe, mg/g</i>	17.0	20.7	55.1
<i>Mn, mg/g</i>	0.56	1.97	1.27
As, $\mu\text{g/g}$	35.8	41.6	137.5
Cd, $\mu\text{g/g}$	0.4	0.2	0.5
Co, $\mu\text{g/g}$	17.2	17.1	32.9
Cr, $\mu\text{g/g}$	64.1	60.6	102.6
Cu, $\mu\text{g/g}$	82.9	53.6	113.8
Ni, $\mu\text{g/g}$	61.2	55.9	107.5
Pb, $\mu\text{g/g}$	18.6	19.5	43.1
Th, $\mu\text{g/g}$	10.5	13.2	14.0
U, $\mu\text{g/g}$	4.3	3.6	4.7
Zn, $\mu\text{g/g}$	62.5	98.8	170.3
<b>TC*, % w/w</b>	<b>2.64</b>	<b>3.1</b>	<b>6.2</b>
<b>IC*, % w/w</b>	<b>&lt;0.014</b>	<b>&lt;0.014</b>	<b>&lt;0.014</b>

\*Analysed by ICP-MS, 10% deviation

♠ Non-detectable, too high concentration

\*TC = total carbon, IC = inorganic carbon, determined by total carbon analyzer.

There are a number of studies reporting that the overburden soil containing pyrite and sulfide minerals can generate acidic wastewater, the so called acid mine drainage (AMD) (93, 97-98). The AMD is produced by natural leaching of the mine overburden soil. The AMD contains high amounts of heavy metals because the metals are dissolved in the very acidic leachate solutions. The migration of the metal species in the AMD to the environment is important to be studied. The LN1 sample is chosen to study further the leaching behavior of elements in the contaminated soils since it contains high amounts of pyrite and jarosite phases.

### ***3.1.2 Leaching of the Coal-mining Overburden Soil***

In order to study the release of heavy metals from the soil in a mining area, leaching of the soil sample by artificial rainwater and a humic acid solution (which represents as surface water containing natural organic matter) was performed.

High concentrations of some metal ions, for example Fe, Mn, Al, Zn and Cu were found in the leachate solutions collected from leaching by both artificial rainwater and humic acid solutions (**Figure 3.4**). The metal ions were dissolved in the leachate, which became acidic ( $\text{pH} < 3$ ). The characteristics of the leachate obtained by leaching experiment are similar to those of AMD found in reality, containing also high amount of metal ions (93, 97-98). The main factor, being responsible for the metal ion content and the acidity of the AMD is the presence of pyrite ( $\text{FeS}_2$ ) and other sulfide minerals in the mine disposal (97, 99, 100). Thus, the soil sample was analyzed by X-ray diffraction for some mineral phases. As mentioned before, pyrite

and its oxidation product, jarosite ( $\text{KFe}_3(\text{SO}_4)_2(\text{OH})_6$ ) were found in the LN1 soil sample. Due to the oxidation of pyrite and sulfide minerals under aerobic conditions, sulfuric acid is produced. The acidic solution in turn dissolves a number of minerals and thus relatively high metal ions are released. The humic acid colloids did not affect the leaching of the metals from the soil. The predominant factor controlling metal ion solubility in the leachate is the presence of acid.

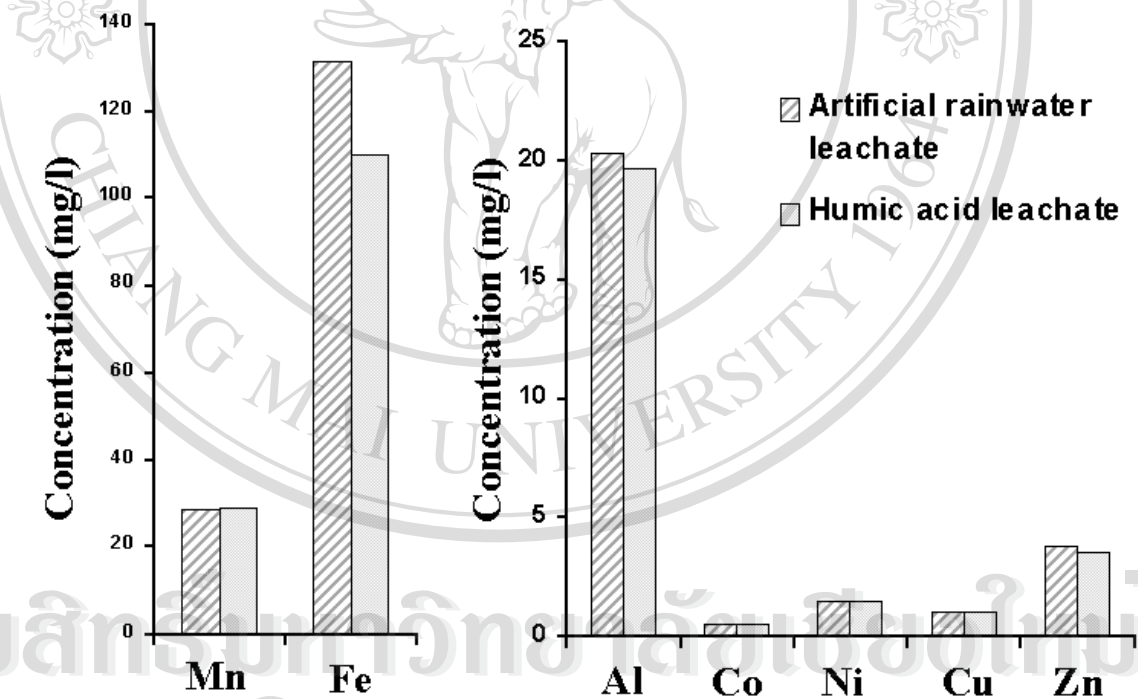


**Figure 3.4** Some heavy metals found in the artificial rainwater and humic acid leachate solutions obtained from leaching of soil sample

### **3.1.3 On-line Size-based Element Speciation**

After the initial leaching of metal ions under the acidic conditions, the heavy metal ions can be further released to the environment by surface water. In surface water with pH values around 7, there are organic colloids, which can associate with metal ions. Thus, to study the association of the metal ions released from the soil in mining area with organic colloids, the leachate collected from the leaching experiment was mixed with humic acid solution at different ratios (1:100, 1:200, 1:300, 1:500 and 1:1000) to simulate the dilution of AMD with surface water of neutral pH. Humic acid colloids were used because it is the most important component of organic matter usually found in surface water.

The AF<sup>4</sup>-ICP-MS system was used to characterize the colloids in the mixture of leachate and humic acid solution. The AF<sup>4</sup> technique gives the information of particle size distribution of colloids whereas the ICP-MS contributes the metal content. Therefore, combination of the AF<sup>4</sup> and ICP-MS provides size-based element speciation.

#### **(A) Colloid Size Distribution in the Mixture of the Leachate and Humic Acid Solution**

A size distribution of the humic colloids in the mixture can be obtained by the AF<sup>4</sup> technique with UV/Vis detection. Size calibration was made by using Latex standard (20, 50 and 100 nm diameter). The obtained calibration equation is  $y=8.7x+441.8$  with correlation coefficient ( $R^2$ ) of 0.9962.

Larger sized particulates were obviously observed in the less diluted leachates with a leachate:humic acid (L:HA) ratio of 1:100, whereas there were no particulates observed in more diluted systems (1:200, 1:300, 1:500 and 1:1000). The sizes of the colloid particles in the L:HA mixtures were calculated and plotted parallel to the elution times as shown in the fractograms (**Figure 3.5**). The fractograms show the shifts of the colloid sizes from smaller size (<5 nm) to larger size (5-10 nm, 10-30 nm, 30-50 nm and 200-450 nm) when the dilution ratio of the L:HA decreases (1:1000, 1:500, 1:300, 1:200 and 1:100, respectively). In other words, a less diluted mixture refers to the higher concentrations of metal ions in the mixture. It indicates that the colloid sizes depend on the concentrations of metal ions. Additionally, the solubility or colloidal stability of HA depends also on pH of the medium. It is insoluble in acid (101). The pH values of the diluted leachate mixtures decreased when the fraction of leachate in the mixture increased. Therefore, for a less dilution ratio (1:100), HA colloids aggregate. The metal ions can associate with the HA aggregates or may even co-precipitate with Fe(III) solid phase. The resulting larger particulates can be partly observed in the fractograms. For a higher dilution ratio (1:200, 1:300, 1:500 and 1:1000), the large particulates were not observed but the smaller-sized colloidal particles are found by AF<sup>4</sup> analysis as described above.

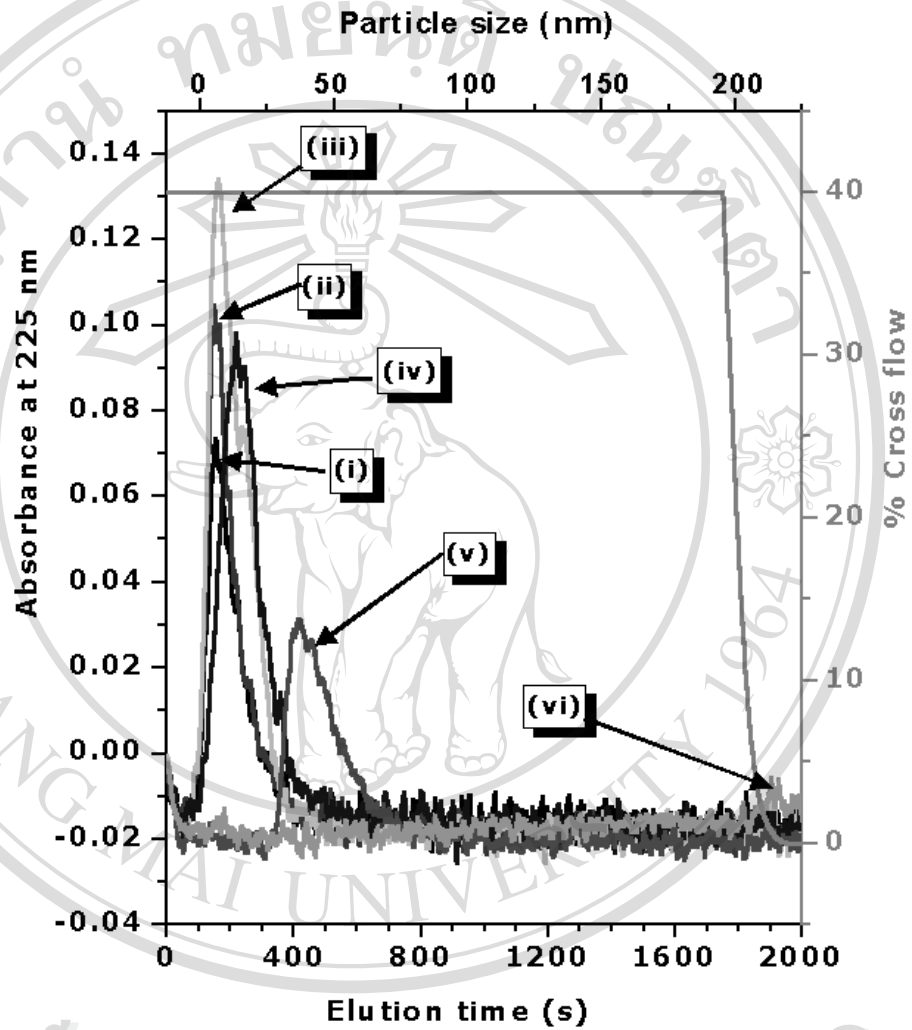


**Figure 3.5** Fractograms of the L:HA mixtures; (i) humic acid solution, pH 6.7, (ii) L:HA=1:1000, pH 6.5, (iii) L:HA=1:500, pH 6.1, (iv) L:HA=1:300, pH 5.6, (v) L:HA=1:200, pH 5.2 and (vi) L:HA=1:100, pH 4.6

## **(B) Metal Ions Associated With Colloids**

### *i) Model System*

Fe(III) is found to be the main component of the soil leachate solutions. In order to define the conditions under which tentatively mobile colloidal species or immobile particulates and precipitates are formed, some experiments are performed with pure Fe(III) and humic acid solutions. Upon dilution of the Fe(III) solution with HA solution, the pH of the mixture increases (**Figure 3.6**). The ratio of Fe(III) to HA is represented as the ratio of Fe(III) ions concentration to the concentration of carboxylate functional groups of the HA. These groups represent the most relevant ligands of HA interacting with the Fe(III). The total concentration of the Fe in all diluted solutions lie close or slightly above the solubility limit of  $\text{Fe}(\text{OH})_3(\text{amorphous})$ . Three days after the diluted solutions were prepared, precipitation was observed at the dilution ratios (mole of Fe(III):equivalents of HA, calculated as mole of  $\text{COO}^-$ ) of 1:1 and 1:2 (pH 3.3 and 3.6). Assuming a co-ordination of 3  $\text{COO}^-$  groups to one Fe(III) ion, HA is overloaded with Fe(III). The loss of DOC, represented as HA content, and Fe(III) concentration from those solutions (**Figure 3.7**) indicated that the Fe(III) phase was precipitated with HA. At the lower Fe(III) to HA ratios (1:3, 1:5 and 1:10), the Fe(III)-HA compounds appear to be stabilised as colloids. The PCS results showed large particles at the lower Fe(III):HA ratio samples (**Figure 3.6**). At the ratio of Fe(III) to HA ( $\text{COO}^-$  functional groups) higher than 1:3, the complexes or colloids start to aggregate and the larger particles, and finally precipitates are formed.

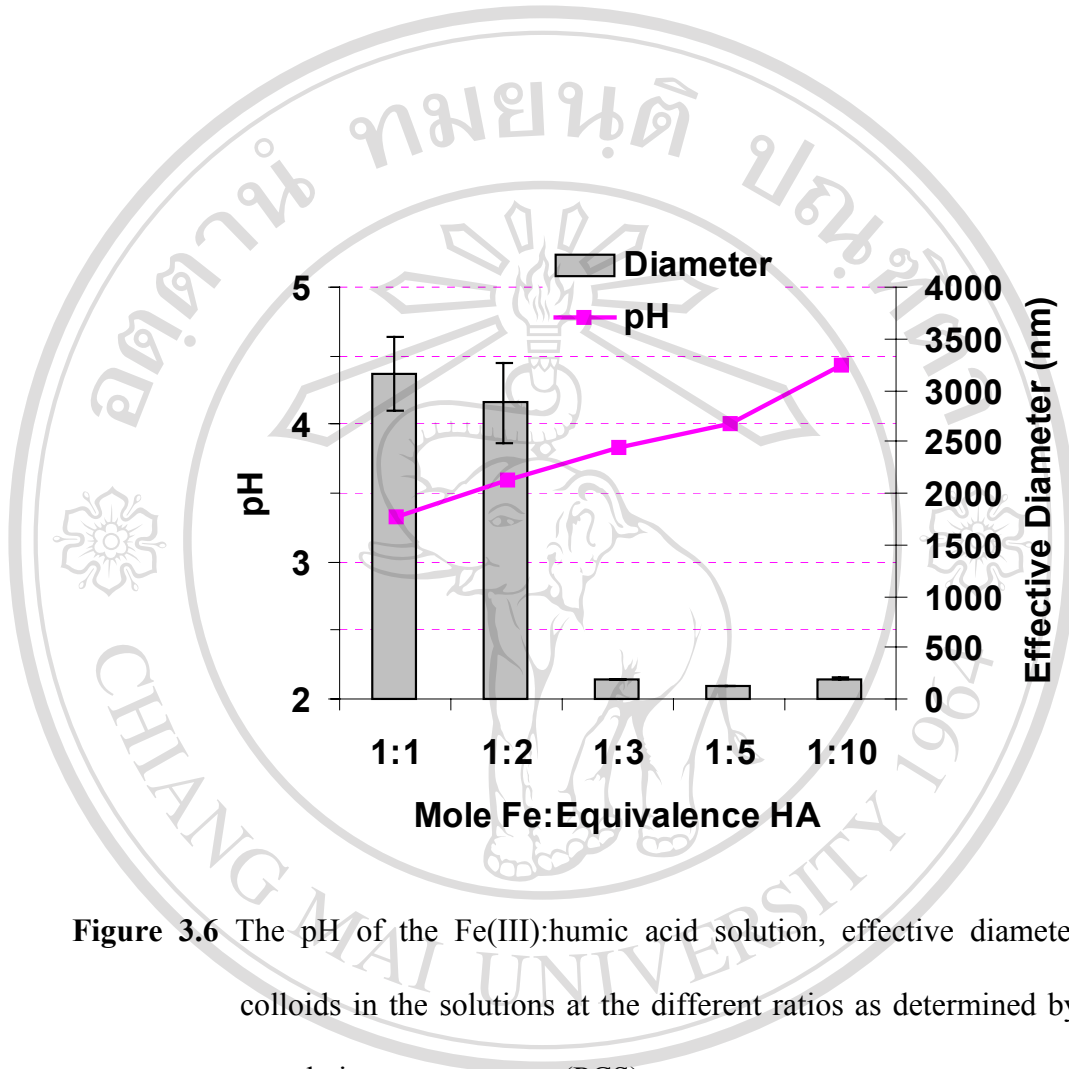


**Figure 3.6** The pH of the Fe(III):humic acid solution, effective diameter of the colloids in the solutions at the different ratios as determined by photon correlation spectroscopy (PCS)

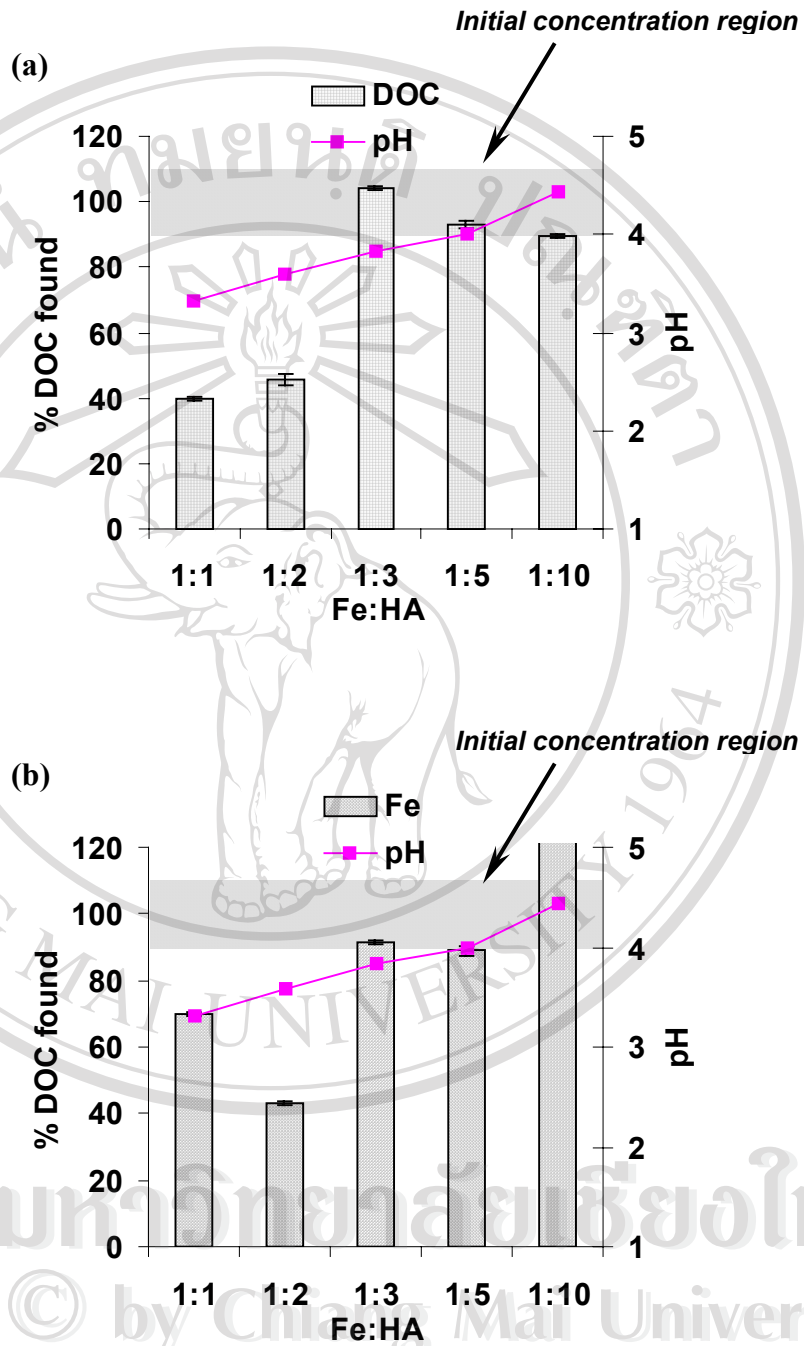


**Figure 3.7** Dissolved organic carbon (DOC) and Fe concentration in the diluted Fe(III)-humic acid solutions

Two parameters, pH and Fe(III):HA ratio, were varied within the dilution experiments. In order to differentiate the influence of both parameters, the experiments are repeated at fixed pH values (**Figure 3.8 and 3.9**). It turns out that both, the presence of Fe(III) at high concentration and the low pH induce agglomeration and precipitation of HA. The highest degree of HA agglomeration and precipitation is observed at pH=2. Decreasing the Fe(III) concentration below a Fe(III)/COO<sup>-</sup> ratio of 1:4 stabilizes the HA in solution even at the low pH at least for the experimental observation period. At pH 6 and 7, the HA remains dissolved even at high Fe(III)/COO<sup>-</sup> ratio after centrifugation of the solution.

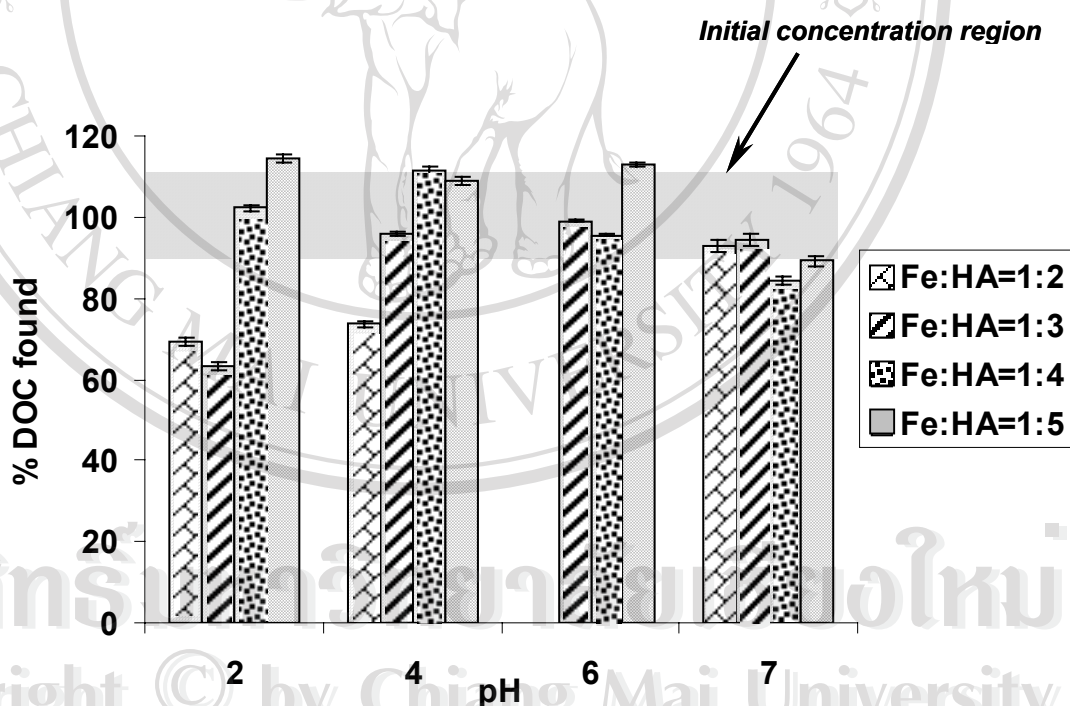


**Figure 3.8** DOC in the Fe(III):humic acid solution at different pH values

The behavior of Fe(III) (**Figure 3.9**) does not reveal such a clear trend. This may be due to (i) the difficulty of determining Fe by ICP-MS where a number of

interferences appear and (ii) due to the tendency of Fe(III) to form colloidal  $\text{Fe}(\text{OH})_3$  species, which are not separated by centrifugation. Both facts are thought to be responsible for the unclear pattern observed for the Fe(III) behavior in **Figure 3.9**.

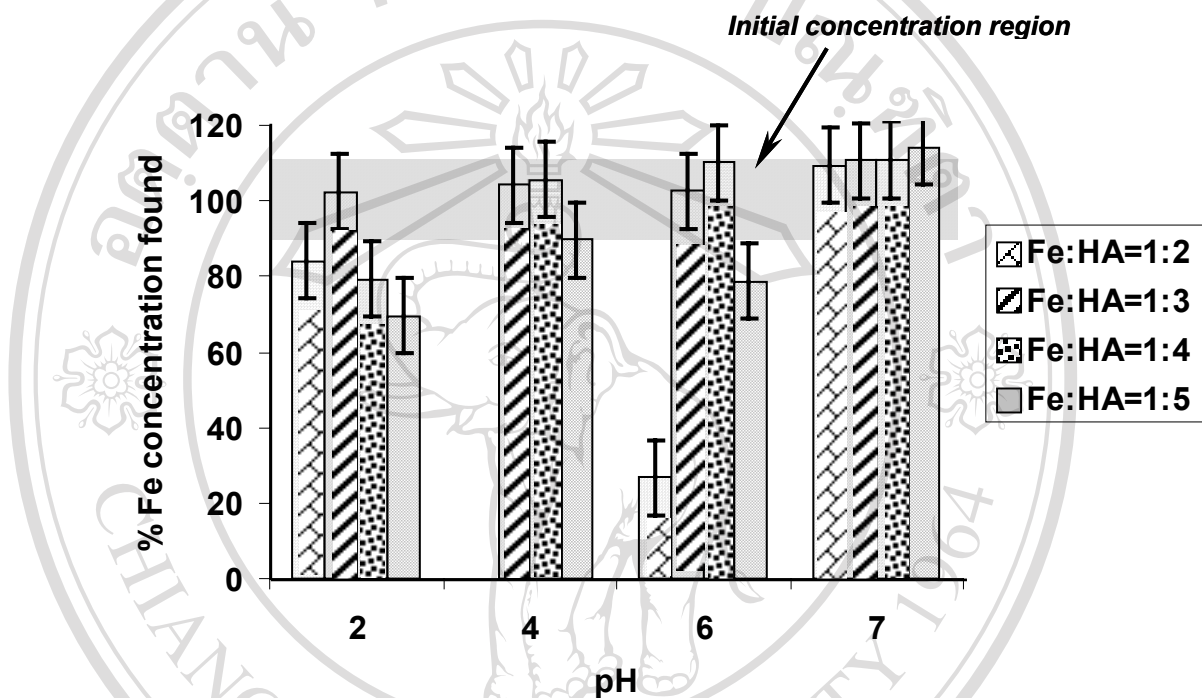


**Figure 3.9** Fe concentration in the Fe(III):humic acid solution at the different pH values

From these experiments it is concluded that at  $\text{pH} > 4$  and a  $\text{Fe}/\text{COO}^-$  ratio  $< 1:3$  formation of stable colloids are likely. Solutions with higher pH and higher Fe(III) concentrations may at least partly cause precipitation of a major part of HA. The influence of other dissolved ions as  $\text{Na}^+$  and  $\text{Ca}^{2+}$  may also affect humic colloid stability but are not considered here as their concentration in the leachate is comparatively low.

*ii) Artificial System*

The distribution of metal ions in colloidal particles when diluting the leachate solution with HA solution was obtained by AF<sup>4</sup>-ICP-MS. The ICP-MS results (**Figure 3.10**) show the similar trends as found in the fractograms in **Figure 3.5**, i.e. a longer elution time appears for the less diluted mixtures. It illustrates the shift of the particle sizes from the smaller (<5 nm) to the larger diameter. The signal obtained from the ICP-MS refers to the metal content in the sample. Thus, it can be interpreted that some metal ions, for examples Fe, Al, Cu and Eu, are associated with humic acid colloids in all sample solutions. Even the HA solution without leachate contains those metal ion contents. As it can be seen in the case of Al, at the ratios of 1:300 (pH 5.6), 1:200 (pH 5.2) and 1:100 (pH 4.6), ICP-MS signals higher than those of the humic acid alone in the size range of 50-200 nm were observed. Anyhow, in the same size range, no absorbance signal is observed by the UV detector (**Figure 3.5**). Those particles in the size range of 50-200 nm could be inorganic colloids. Indeed, the pH value influences the formation of inorganic colloids such as hydrous oxides of metal ion (i.e. FeOOH and AlOOH) (102, 103). At pH 4-5, these inorganic colloids are likely to occur (103). It could be the reason for the signal obtained in the size range of 50-200 nm by the AF<sup>4</sup>-ICP-MS. The results from AF<sup>4</sup>-ICP-MS show a peak after the cross-flow was no longer applied (after an elution time of 1800 s). UV detection does not provide a signal here. It indicates that the eluted fraction after the elution time of 1800 s contains the larger-sized inorganic colloids stabilized by the humic acid coating. These findings indicate that the leached metal ions from the mine disposal

soil sample could be associated with mobile humic acid colloids or immobile larger aggregates depending on the metal ion to humic acid concentration ratio and pH.

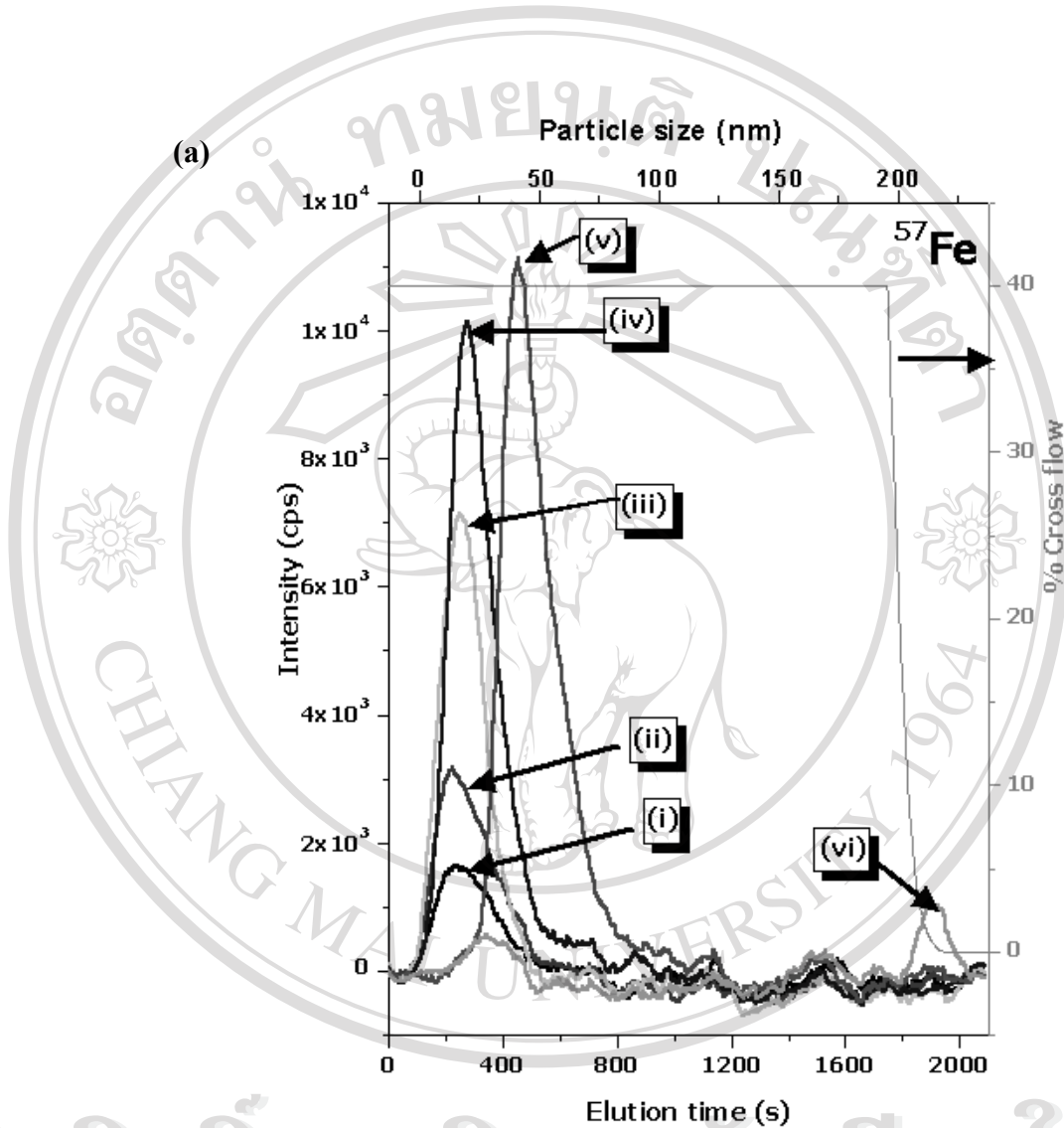


**Figure 3.10 (a)** Fe distributions on humic acid colloids characterized by the AF<sup>4</sup>-ICP-MS system; (i) humic acid solution, pH 6.7, (ii) L:HA=1:1000, pH 6.5, (iii) L:HA=1:500, pH 6.1, (iv) L:HA=1:300, pH 5.6, (v) L:HA=1:200, pH 5.2 and (vi) L:HA=1:100, pH 4.6

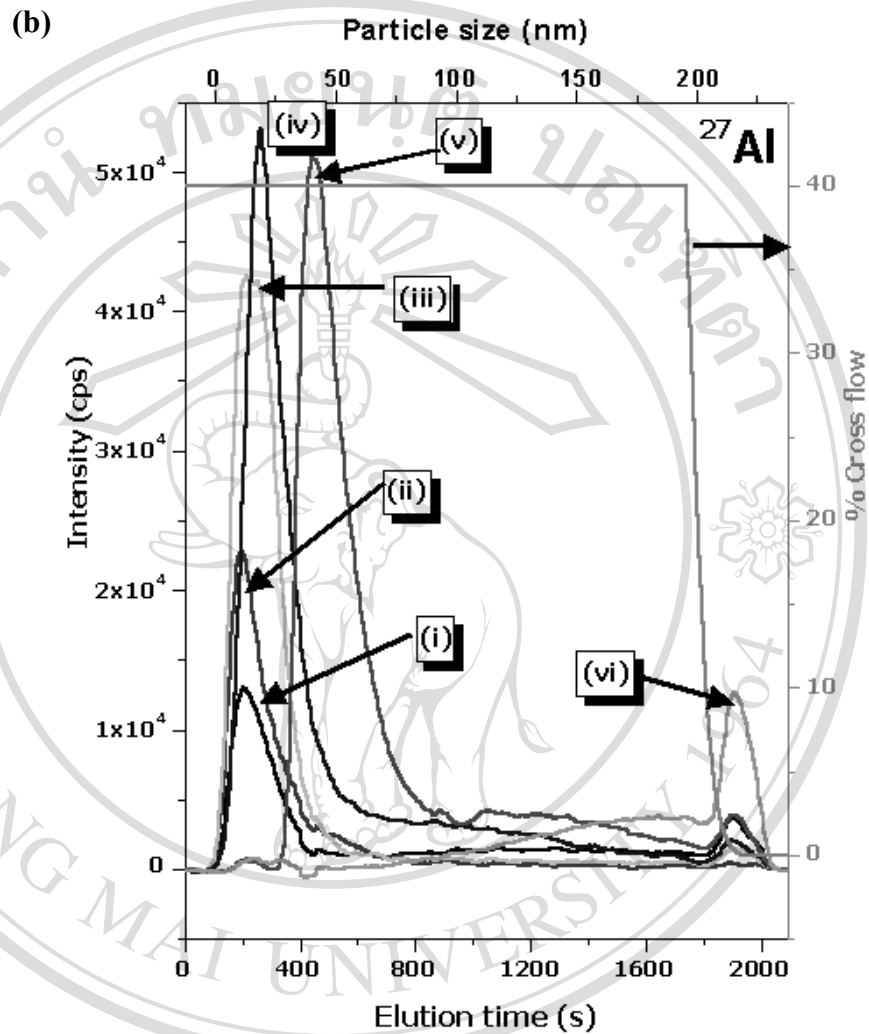


**Figure 3.10 (b)** Al distributions on humic acid colloids characterized by the AF<sup>4</sup>-ICP-

MS system; (i) humic acid solution, pH 6.7, (ii) L:HA=1:1000, pH 6.5,

(iii) L:HA=1:500, pH 6.1, (iv) L:HA=1:300, pH 5.6, (v) L:HA=1:200,

pH 5.2 and (vi) L:HA=1:100, pH 4.6

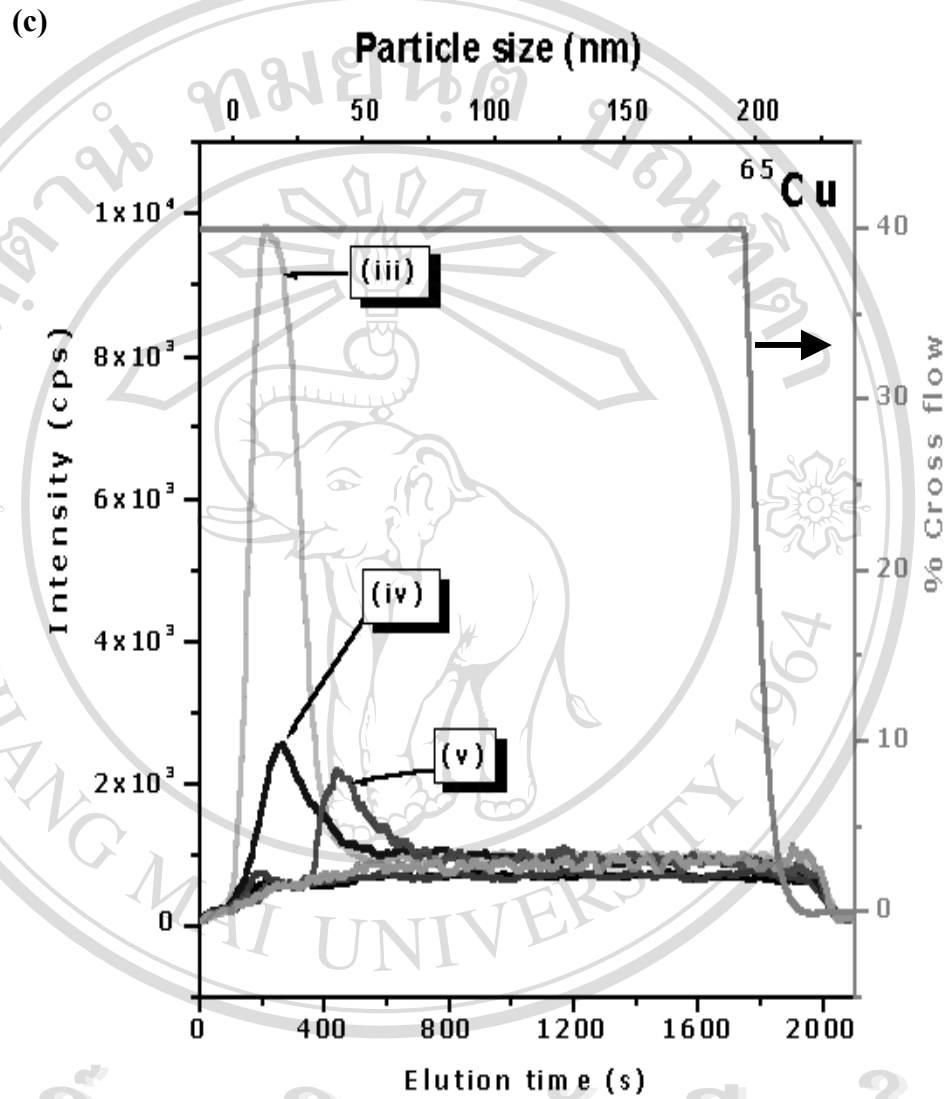


**Figure 3.10 (c)** Cu distributions on humic acid colloids characterized by the AF<sup>4</sup>-ICP-MS system; (i) humic acid solution, pH 6.7, (ii) L:HA=1:1000, pH 6.5, (iii) L:HA=1:500, pH 6.1, (iv) L:HA=1:300, pH 5.6, (v) L:HA=1:200, pH 5.2 and (vi) L:HA=1:100, pH 4.6

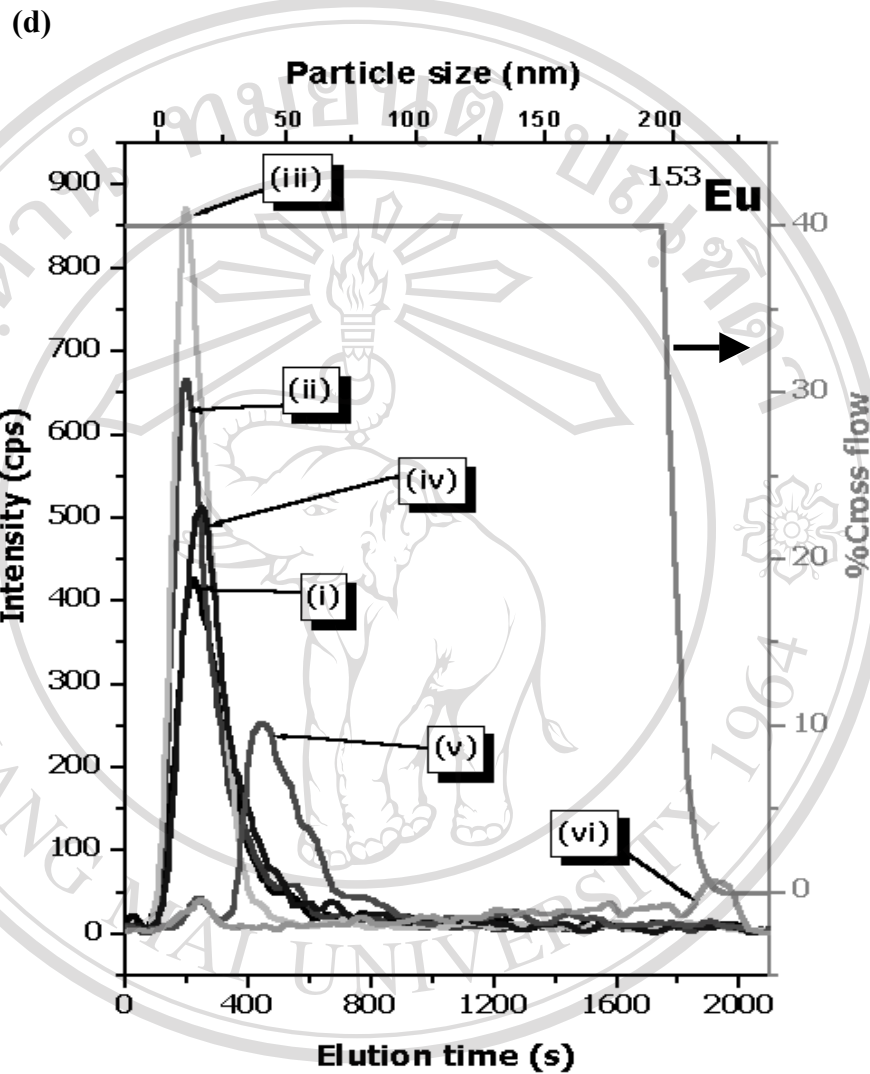


**Figure 3.10 (d)** Eu distributions on humic acid colloids characterized by the AF<sup>4</sup>-

ICP-MS system; (i) humic acid solution, pH 6.7, (ii) L:HA=1:1000, pH

6.5, (iii) L:HA=1:500, pH 6.1, (iv) L:HA=1:300, pH 5.6, (v)

L:HA=1:200, pH 5.2 and (vi) L:HA=1:100, pH 4.6

### 3.2 Development of the Flow Injection Analysis-Anodic Stripping Voltammetry

In order to analyze the dissolved forms of elements in the leachate solution from the leaching of the contaminated soil, flow-based analysis (FBA) systems, i.e. flow injection analysis (FIA) and sequential injection analysis (SIA), coupled with anodic stripping voltammetric (ASV) detection system were developed. The former system (flow injection analysis-anodic stripping voltammetry (FIA-ASV)) was developed first. The SIA-ASV system was developed later by adopting the experience from developing the FIA-ASV system.

A mercury film electrode (MFE) was used as the working electrode (WE) throughout this work. The preplated MFE was prepared on-line so that the mercuric solution waste can be stored separately and thus can be handled easily. Moreover, preparing the MFE by on-line preplating method reduced the amount of mercuric waste.

#### 3.2.1 On-line Preparation of Mercury Film Electrode

The preparation of the mercury film electrode (MFE) for the use with the developed FIA-ASV system was studied. Hg(II) concentrations of 500 and 1000 mg/l were tested. The mercury film (MF) was coated fully on the glassy carbon electrode (GCE) by using 500 mg/l Hg(II), whereas using 1000 mg/l Hg(II) yielded incomplete coating on the GCE. It could be explained that the concentration of the Hg(II) ion was too high and the amount of deposited Hg was too much. Therefore, part of the MF may peel off during deposition. Deposition potentials of  $-0.8$ ,  $-0.9$  and  $-1.0$  V vs

Ag/AgCl RE were studied. It was found that mercury was adsorbed on the GCE at a potential of  $-0.8$  V. At the deposition potential of  $-0.9$  and  $-1.0$  V, mercury could not be coated on the GCE because  $H^+$  ion in the solution was reduced at the GCE and prevented the MF formation. Higher peak currents for the metals were obtained when using the MFE plated with a deposition time of 10 min. However, MF deterioration was observed because mercury did not adhere strongly to the glassy carbon and resulted in rapid decrease in sensitivity. Therefore, the MF was cleaned electrochemically at a potential of 0 V for 20 s before performing the next run. The proposed MF conditions have been experimentally tested. The MF was prepared on-line (in the closed system). Thus the preplated MF was prevented from oxidation by oxygen. That resulted in reusing the on-line preplated MFE for more than 80 analysis cycles (as shown in **Figure 3.11**).

Using the preplated MFE, there are many advantages over using the hanging mercury drop electrode (HMDE), which has been used for years. Firstly, it is safer to work with the MFE than to work with the mercury drop because mercury is known to form very toxic vapor. Thus, using the MFE prevents the operator from mercuric vapor. Secondly, the mercuric solution waste from the preparation by on-line preplating can be kept separately. It is easier to handle the mercuric solution waste than to deal with elementary mercury. In addition, using the MFE also gives higher sensitivity than using mercury drop because the MFE offers a higher surface-to-volume ratio (16).

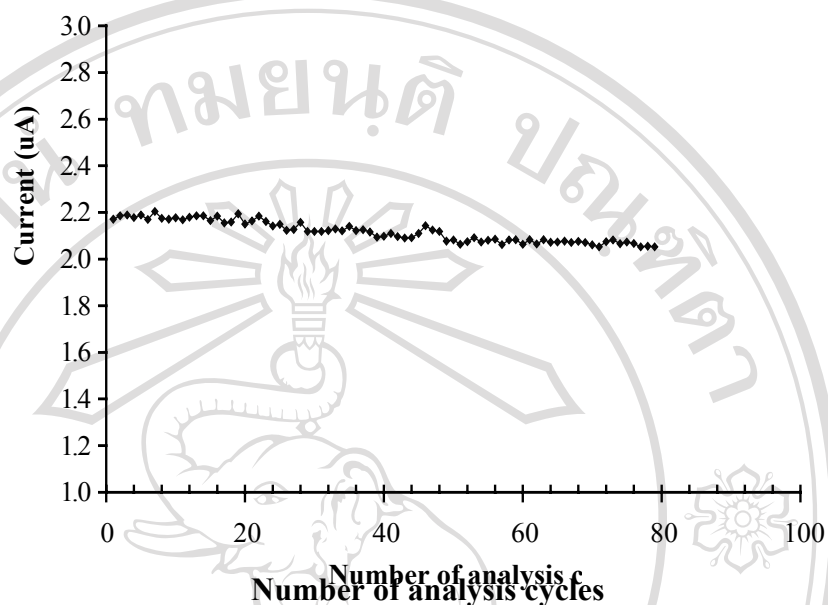


**Figure 3.11** Stability of the on-line preplated mercury film electrode illustrating by the current of 100  $\mu\text{g/l}$  Cd(II)

### 3.2.2 Optimization of the FIA-ASV system

The FIA-ASV system can be assembled easily as depicted in **Figure 2.3**. A single line of acetate buffer solution was used as a carrier. Optimization of the FI parameters was performed.

#### A) Acetate Buffer Concentration

Electrolyte concentration affects the ionic strength of the solution and hence the peak currents of metal ions. Concentrations of acetate buffer solution (0.1, 0.2,

0.3, 0.5, 0.7 and 1.0 mol/l) were varied while the other parameters were fixed. 0.5 mg/l Zn(II) were used for testing. It was found that the peak currents fluctuated at an acetate buffer concentration less than 0.5 M as shown in **Figure 3.12**. Obviously, the ionic strength of the less concentrated buffer solution was not sufficient. A concentration of 0.6 mol/l acetate buffer was chosen.

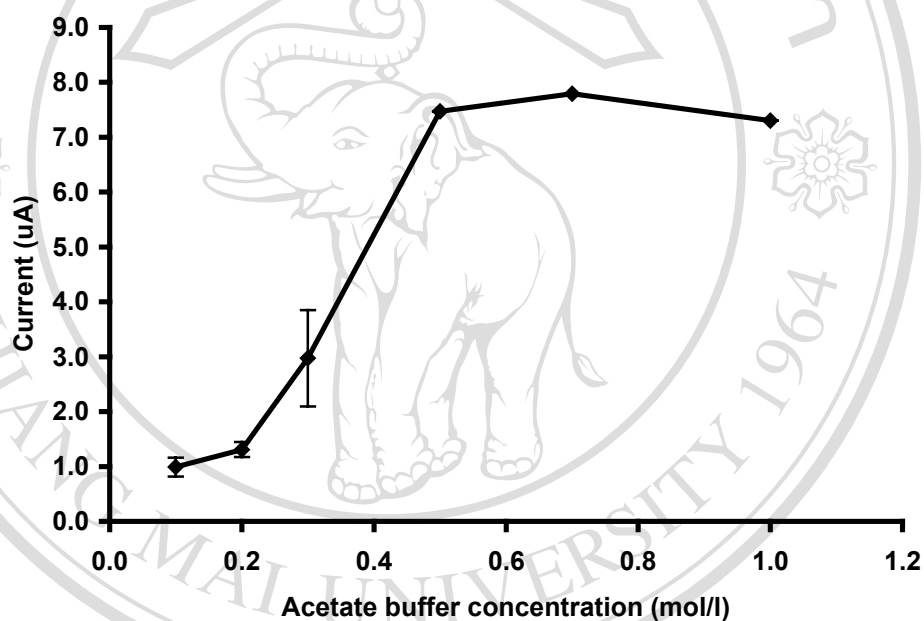


**Figure 3.12** Effect of acetate buffer concentration

### ***B) Sample Volume***

The optimum sample volume to be injected depends on carrier flow rate and deposition time. At a deposition time of 20 s and a flow rate of 0.5 ml/min, approximately 167  $\mu\text{l}$  of sample are required. To study the effect of injected sample volume, Zn(II) solution was analyzed. Injection volumes of 30, 80 and 130  $\mu\text{l}$  were tested. It was found that the sensitivity obtained by using a volume of 30  $\mu\text{l}$  was not different from that obtained by using a volume of 80  $\mu\text{l}$  (see **Figure 3.13**). However, using an injection volume of 130  $\mu\text{l}$  yielded the lowest current. Injecting larger sample volumes obviously impedes the optimal mixing of the sample and electrolyte solution. The precision of the currents obtained by introducing a 30  $\mu\text{l}$  sample volume was found to be the best. Under these conditions the sample/buffer mixing is quantitative and thus better reproducibility for the current is observed. Using a sample volume of 30  $\mu\text{l}$  also resulted in satisfactory current. Therefore, the injection volume of 30  $\mu\text{l}$  was fixed.

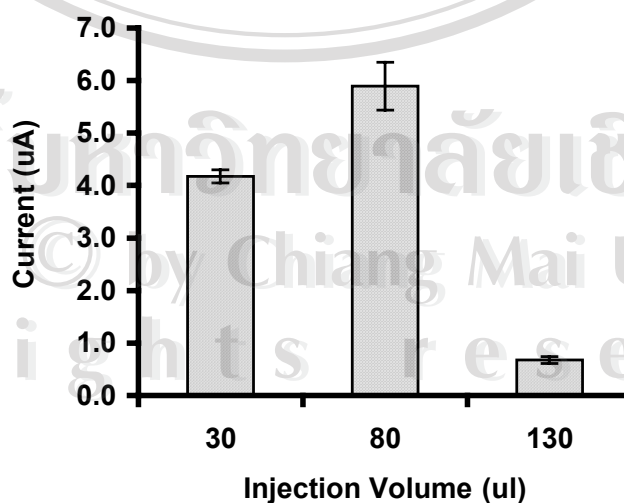


**Figure 3.13** Effect of sample volume

### C) Flow Rate

The effect of carrier flow rate was studied by using Cd(II) and Pb(II) as representative metal ions at a concentration of 100  $\mu\text{g/l}$ . As expected, peak currents of metals increased when the flow rate increased (**Figure 3.14**). The higher flow rate improves the deposition of metal ions at the MFE. Since the reduction of metal ions at the MF surface is diffusion controlled, the higher flow rate directly targeted to the MF surface certainly improves the metal ion transport to the MFE, and thus the enrichment efficiency. However, at a higher flow rate than 0.5 ml/min, the MFE deteriorates. Thus, the flow rate of 0.5 ml/min was used in this FIA-ASV system.

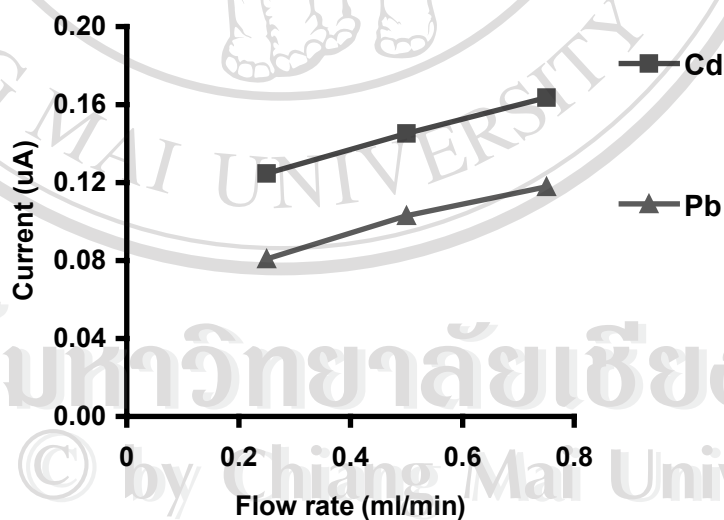


**Figure 3.14** Effect of flow rate

#### D) Mixing Coil Length

Mixing coil lengths of 50, 100 and 150 cm were tested. The results (**Figure 3.15**) show that using the mixing coil of 100 cm long provides a higher signal than using the other lengths. However, for the low flow rate employed (0.5 ml/min), a mixing coil length of 50 cm was used so that a compromise on high sample throughput, good reproducibility and optimal signal height could be achieved.

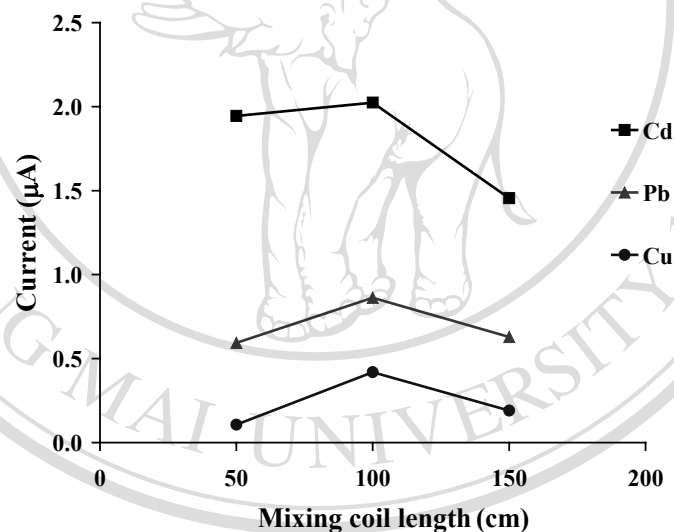


**Figure 3.15** Effect of mixing coil length

### 3.2.3 Performance of the Developed FIA-ASV System

Voltammograms of metal standards obtained by the FIA-ASV system are depicted in **Figure 3.16**. Peak potentials ( $E_p$ ) of Zn(II), Cd(II), Pb(II) and Cu(II) ions are  $-0.95 \pm 0.03$  V,  $-0.55 \pm 0.03$  V,  $-0.39 \pm 0.03$  V and  $0.03 \pm 0.03$  V, respectively. Calibration data, detection limits (defined as in (104)), and precisions (as %RSD,  $n=11$ ) for the analysis of metal ions are summarized in **Table 3.3**. The results illustrate that simultaneous determination of Zn(II), Cd(II), Pb(II) and Cu(II) can be performed by using the developed FIA-ASV system with a sample throughput of 20  $h^{-1}$  and with good sensitivity.

The proposed FIA-ASV system is a single line FI system. Thus, it is very easy to set up. This FIA-ASV system consumes less amounts of reagents and samples than batch ASV system. It is safe for the operator because it is a closed system. The working electrode used in this work is the MFE, which produces no mercuric vapor like the mercury drop electrode does. Moreover, it shows the possibility of further development of other flow-based systems.

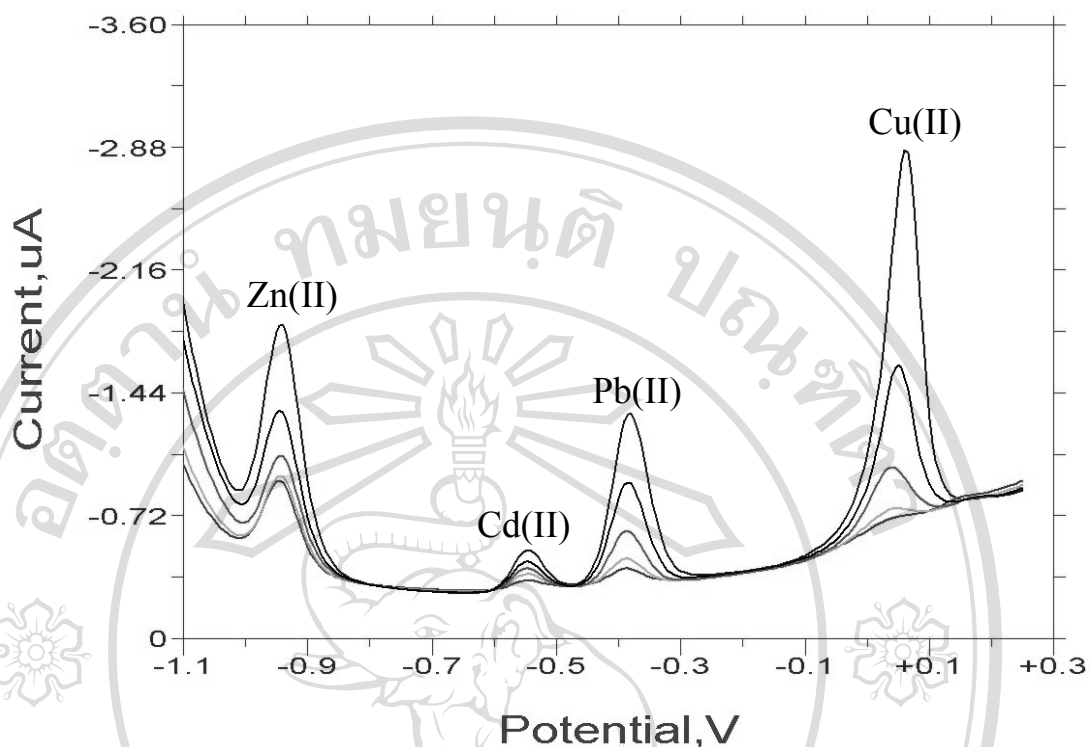


**Figure 3.16** Voltammograms of metal standards obtained by the FIA-ASV system (concentration of Zn(II), Pb(II), Cu(II): 10, 20, 50, 100 and 200  $\mu\text{g/l}$ , and Cd(II): 5, 10, 15, 20 and 30  $\mu\text{g/l}$ )

**Table 3.3** Summary of calibration data obtained by the FIA-ASV system

Metal ion	Dynamic range ( $\mu\text{g/l}$ )	Equation	$R^2$	Detection limit * ( $\mu\text{g/l}$ )	%RSD, n=11
Zn(II)	50-200	$Y=4.338x - 0.05$	0.9440	17	4.3 % at 100 $\mu\text{g/l}$
Cd(II)	10-30	$Y=6.667x + 0.02$	0.9990	1	3.6 % at 10 $\mu\text{g/l}$
Pb(II)	10-100	$Y=5.466x + 0.02$	0.9997	2	1.8 % at 80 $\mu\text{g/l}$
Cu(II)	20-200	$Y=11.569x - 0.19$	0.9962	18	4.4 % at 75 $\mu\text{g/l}$

\* defined as in (104)

### 3.2.4 Application to Model Samples

The developed FIA-ASV system should in principle be able to be applied for the operational speciation of strongly complexed (or colloid-borne) metal ions and free ionic species. However, due to time constraint, the FIA-ASV system was first tested to determine some metal ions, i.e. Zn(II), Cd(II), Pb(II) and Cu(II), in model samples that did not contain any interferences (drinking water samples). The drinking water samples (6 samples) were directly injected into the FIA-ASV system for the simultaneous determination of Zn(II), Cd(II), Pb(II) and Cu(II) ions. The developed FIA-ASV system was also applied to analyze the metals in wastewater samples (3 samples) collected from a stream near an industry. The wastewater samples were treated by UV-digestion using a homemade UV digester. The analysis results of the wastewater samples obtained by using the FIA-ASV system were compared to those obtained by using electrothermal atomic absorption spectrophotometry (ETAAS).

Metal ions in six drinking water samples were analyzed by the FIA-ASV system. The metals in those samples were found to be below the detection limits. This indicates that the metal concentrations in the drinking water samples were below the values of the maximum allowance of 500 mg/l, 0.01 mg/l, 0.1 µg/l and 1.0 mg/l for Zn(II), Cd(II), Pb(II) and Cu(II), respectively (105). The wastewater samples were digested for 2 hrs by using a homemade UV digester (Figure 2.5). UV-digestion can reduce some interferences in such samples as illustrated in Figure 3.17. Well-defined voltammetric peaks of metals were obtained for a sample pretreated by UV-digestion. Results are summarized in Table 3.4. The samples were also analyzed by ET-AAS. The results obtained from the FIA-ASV method agreed with those obtained from ET-

AAS. Zn and Cu may form an intermetallic Zn-Cu phase in MF, which may cause variation in FIA-ASV results of these metals (27,106).

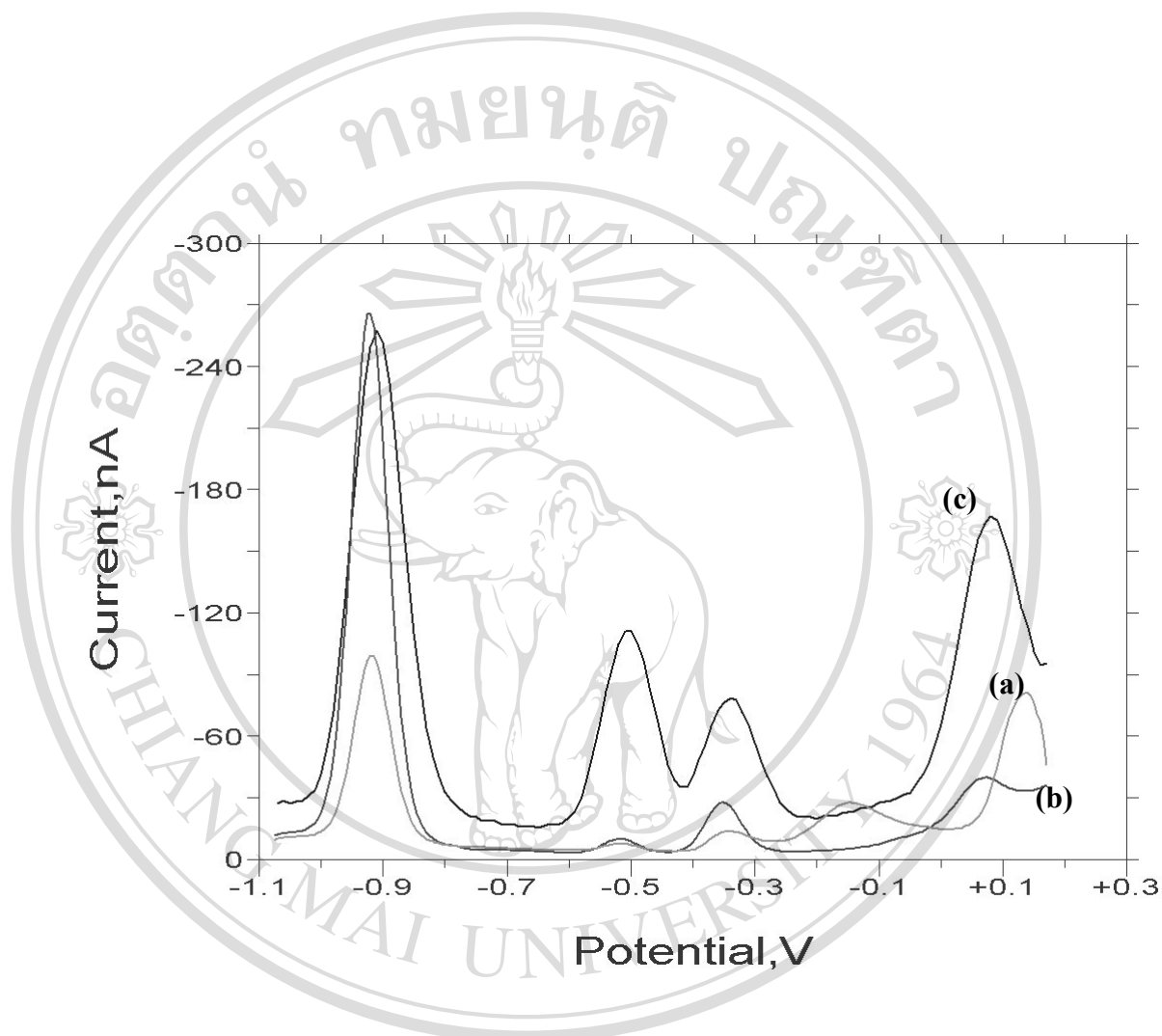


**Figure 3.17** Compared voltammograms of samples; (a) without UV-digestion, (b) with UV-digestion and (c) a standard solution

**Table 3.4** Analyses of model samples by the FIA-ASV system

Sample No.	Concentration found ( $\mu\text{g/l}$ )							
	Zn(II)		Cd(II)		Pb(II)		Cu(II)	
	FIA-ASV	ETAAS	FIA-ASV	ETAAS	FIA-ASV	ETAAS	FIA-ASV	ETAAS
1	154	142	26	25	92	95	60	75
2	74	155	54	50	196	204	115	153
3	45	25	4	7	28	24	27	22

### 3.3 Development of the Sequential Injection Analysis-Anodic Stripping Voltammetry (SIA-ASV) System

SIA is well known for low reagent consumption, precision, robustness, and capability of a high degree in automation and the possibility of performing on-line standard addition. In this work, SIA was considered to be combined with ASV for the determination of Zn(II), Cd(II), Pb(II) and Cu(II). The combined SIA-ASV was expected to reduce the consumption of reagents even more than the FIA-ASV system.

### 3.3.1 Preliminary Study of the SIA-ASV System

For the development of the SIA-ASV system, experiences from working with the FIA-ASV system were adopted. A preliminary SIA-ASV system (referred to the SIA-ASV system *I*) was assembled. An existing autotitrator was used as a pumping unit for economic reasons. Acetate buffer solution, 0.6 mol/l pH 4.6, was used as a carrier, similar to the FIA-ASV system, for testing the performance of the SIA-ASV system. Similar conditions as for the FIA-ASV system were applied. The aspiration volume of the available autotitrator was limited to at least 100  $\mu\text{l}$ . Therefore, the sample volume used in this preliminary system had to be  $\geq 100 \mu\text{l}$ . A sample volume of 130  $\mu\text{l}$  was used in the SIA-ASV system *I*.

The dispensed volume had to be optimized in order to synchronize with the deposition step. Starting the deposition step at a volume of 0.30 ml or at a time of 36 s after starting dispensing the sample zone to the detector, the highest peak current was observed. Simultaneous determination of Zn(II), Cd(II), Pb(II) and Cu(II) can be performed by using the SIA-ASV system. The voltammograms of the metal ions are illustrated in **Figure 3.18**. The results in **Table 3.5** shows that the SIA-ASV system provides linear calibrations with good correlations, low detection limits and satisfactory precisions (as %RSD, n=11) for the metal ions, except the detection limit for Zn(II) was high because of its low sensitivity. The observed low sensitivity of Zn(II) could be due to the intermetallic of Zn-Cu (27, 106). Due to the discontinuous nature of SI operation, reagent consumption and waste generation can be further minimized as compared with FIA-ASV.

The performance of the preliminary SIA-ASV system showed the possibility for developing further the SIA-ASV system. However, the autotitrator has to be modified to overcome the problem of the limitation of the aspiration volume.

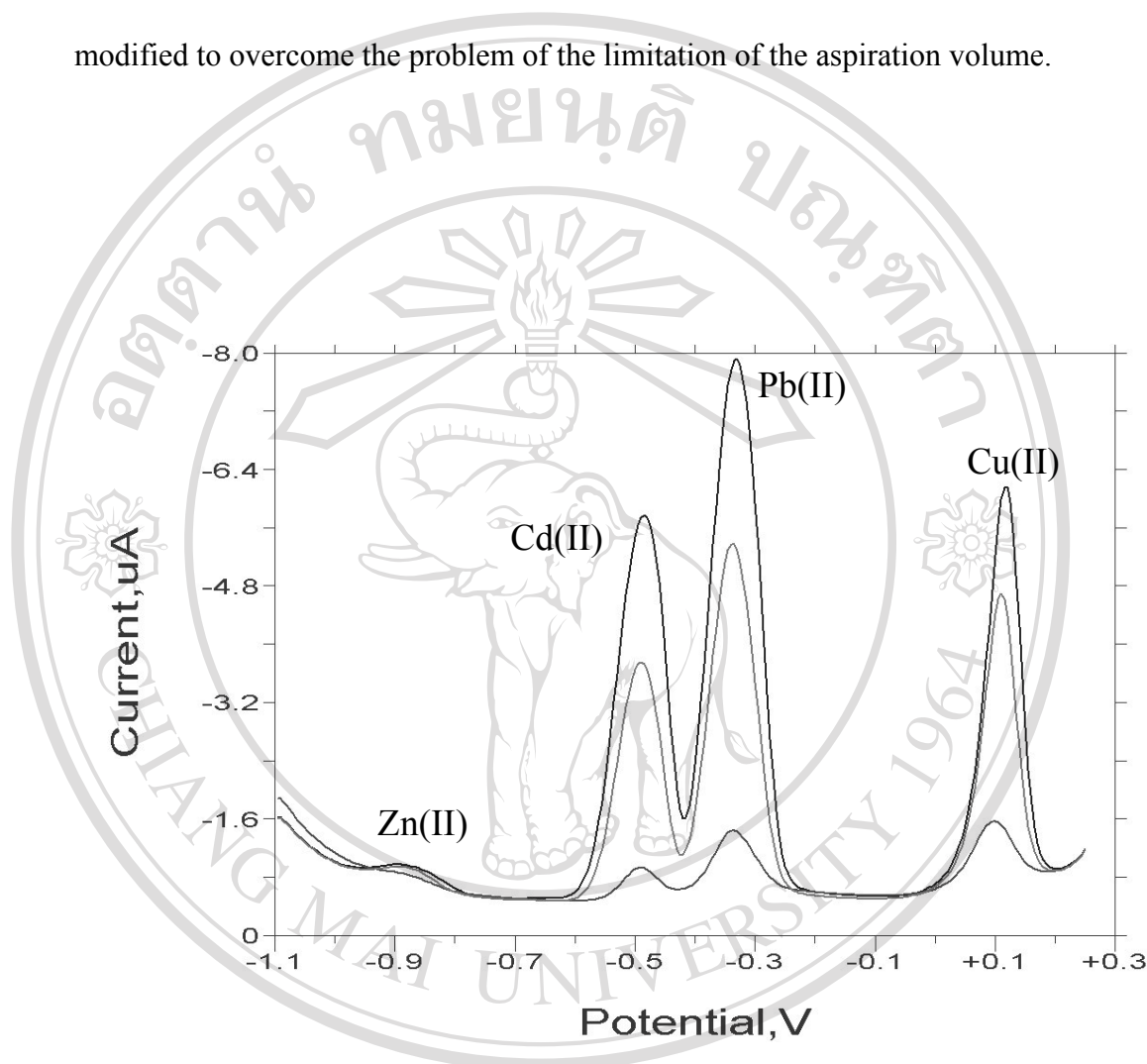


**Figure 3.18** Voltammograms of metal standards obtained by the SIA-ASV system *I* (concentrations of Zn(II): 100, 700 and 1000  $\mu\text{g/l}$ , Cd(II) and Pb(II): 10, 70 and 100  $\mu\text{g/l}$ , Cu(II): 50, 150 and 200  $\mu\text{g/l}$ )

**Table 3.5** Calibration data of the preliminary SIA-ASV system

Metal ion	Dynamic range (µg/l)	Equation	R <sup>2</sup>	Detection limit* (µg/l)	%RSD, n=11
Zn(II)	470-700	$y=0.26x-0.0006$	0.9904	470	0.4 % at 700 µg/l
Cd(II)	10-70	$y=37.47x-0.051$	0.9976	6	10 % at 10 µg/l
Pb(II)	10-100	$y=62.90x-0.191$	0.9946	10	3 % at 40 µg/l
Cu(II)	50-200	$y=29.22x-0.537$	0.9999	3	1 % at 50 µg/l

\* defined as in (104)

### 3.3.2 Development of the SIA-ASV System

The SIA-ASV system *I* worked quite well, except the problem with the limitation of volumes to be aspirated and the use of acetate buffer as the carrier. To assemble an improved SIA-ASV system *II*, the autotitrator was first modified. The modification of the autotitrator should solve the problem with the limited volumes. This drawback was fixed by using the ultrapure water as the carrier and sequentially introducing microliters of reagent at the selection valve instead.

The results obtained by the SIA-ASV system *I* showed the low sensitivity for Zn(II) analysis. It could be because intermetallic Zn-Cu alloy are formed in the MFE (27, 106). Thus, the SIA-ASV system *II* was developed and tested to determine Cd(II), Pb(II) and Cu(II), not Zn(II). The deposition potential in the system *II* was set to  $-0.8$  V, so that Zn(II) was not deposited on the MFE. Zn-Cu intermetallic alloys can thus not form. Moreover, to account for matrix effects in the sample and to reduce

the consumption of standard solution, on-line standard addition was performed. Calculation of metal concentrations using on-line standard addition method will be discussed later on.

#### *A) Modification of Autotitrator*

As a cheaper alternative than the use of a syringe pump in a SI system, an autotitrator (765 Dosimat, Metrohm) was modified as it already consists of a syringe and a plunger, and a carrier bottle, as depicted in **Figure 3.19**. The default 3-way switching valve is replaced by a 3-way solenoid valve (**Figure 3.20**).

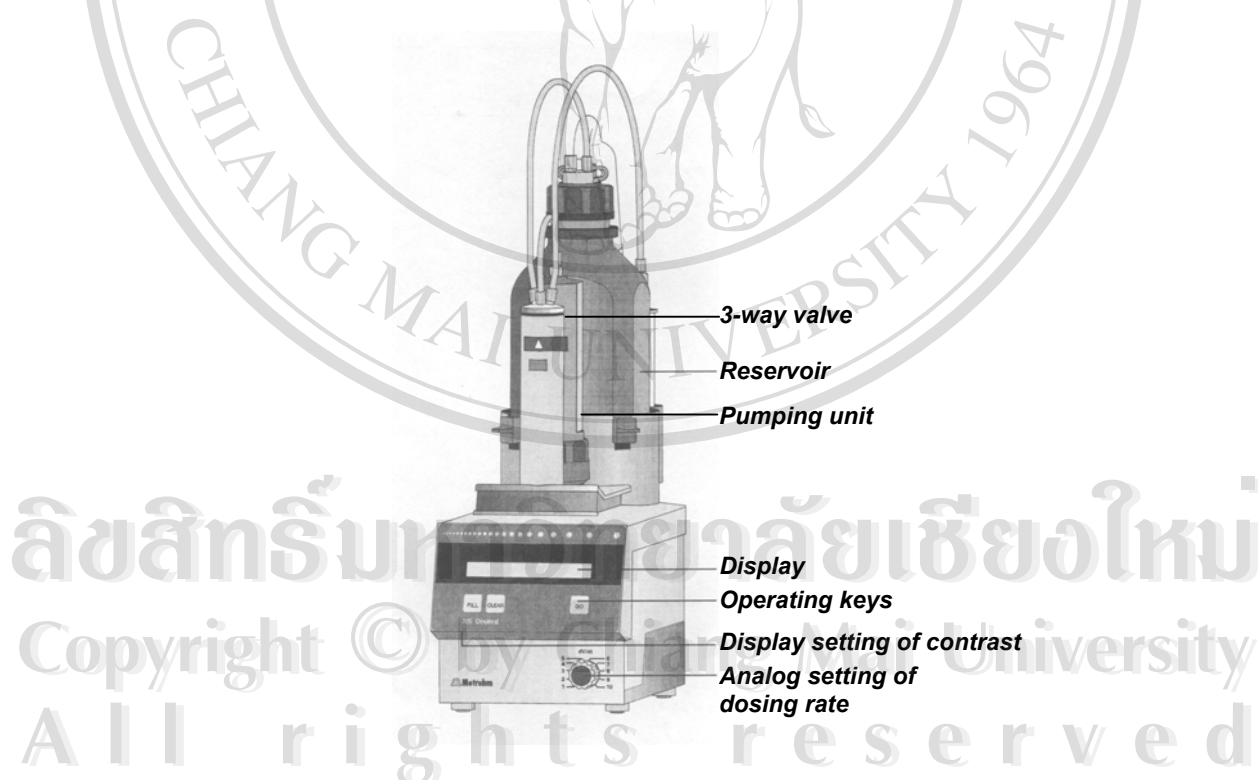


**Figure 3.19** Components of the 665Dosimat autotitrator

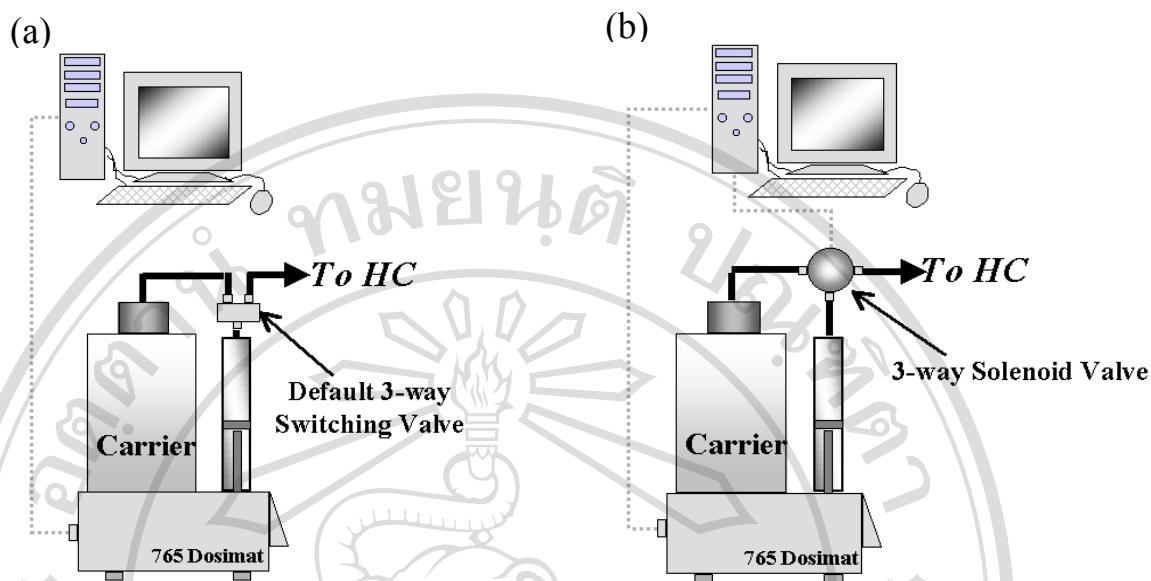
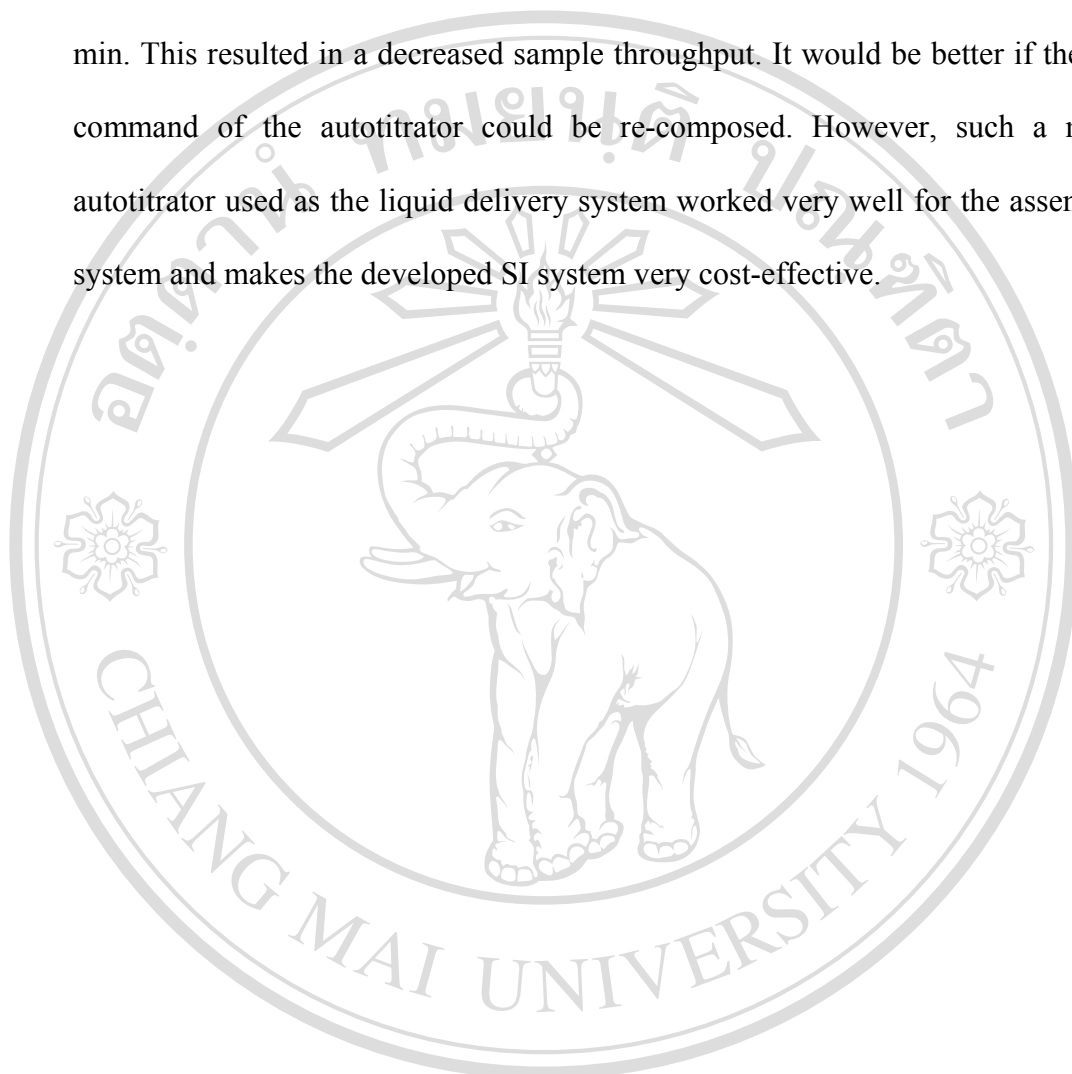


**Figure 3.20** (a) The autotitrator with the default 3-way switching valve

(b) The modified autotitrator with a 3-way solenoid valve

Undesired volume ( $100\ \mu\text{l}$ ) of solution is aspirated to the HC when the autotitrator started to pump a solution (**Figure 3.21(a)**). It is due to the default command of the autotitrator. This limited the free choice of an aspiration volume, which could never be less than  $100\ \mu\text{l}$ . To solve the problem, a 3-way solenoid valve, controlled by the in-house written software, was used instead of the default 3-way selection valve of the autotitrator. The use of the solenoid valve helps circum-venting the undesired volume problem (see **Figure 3.21(b)**). The solenoid valve is switched to the reservoir while the autotitrator is pumping the undesired- $100\ \mu\text{l}$  of solution. By this step, the autotitrator pumped  $100\ \mu\text{l}$  ultrapure water from the reservoir to the syringe. Then the solenoid valve is switched to the other position to aspirate the desired volume to the HC. Due to the default programming command of the autotitrator, it takes a few seconds to initialize the equipment in each step. That

increases analysis time. It should take only ca. 3 min, calculated from the periods required for the individual steps, but the actual time for each measurement was ca. 5 min. This resulted in a decreased sample throughput. It would be better if the default command of the autotitrator could be re-composed. However, such a modified autotitrator used as the liquid delivery system worked very well for the assembled SI system and makes the developed SI system very cost-effective.



ลิขสิทธิ์มหาวิทยาลัยเชียงใหม่  
Copyright © by Chiang Mai University  
All rights reserved

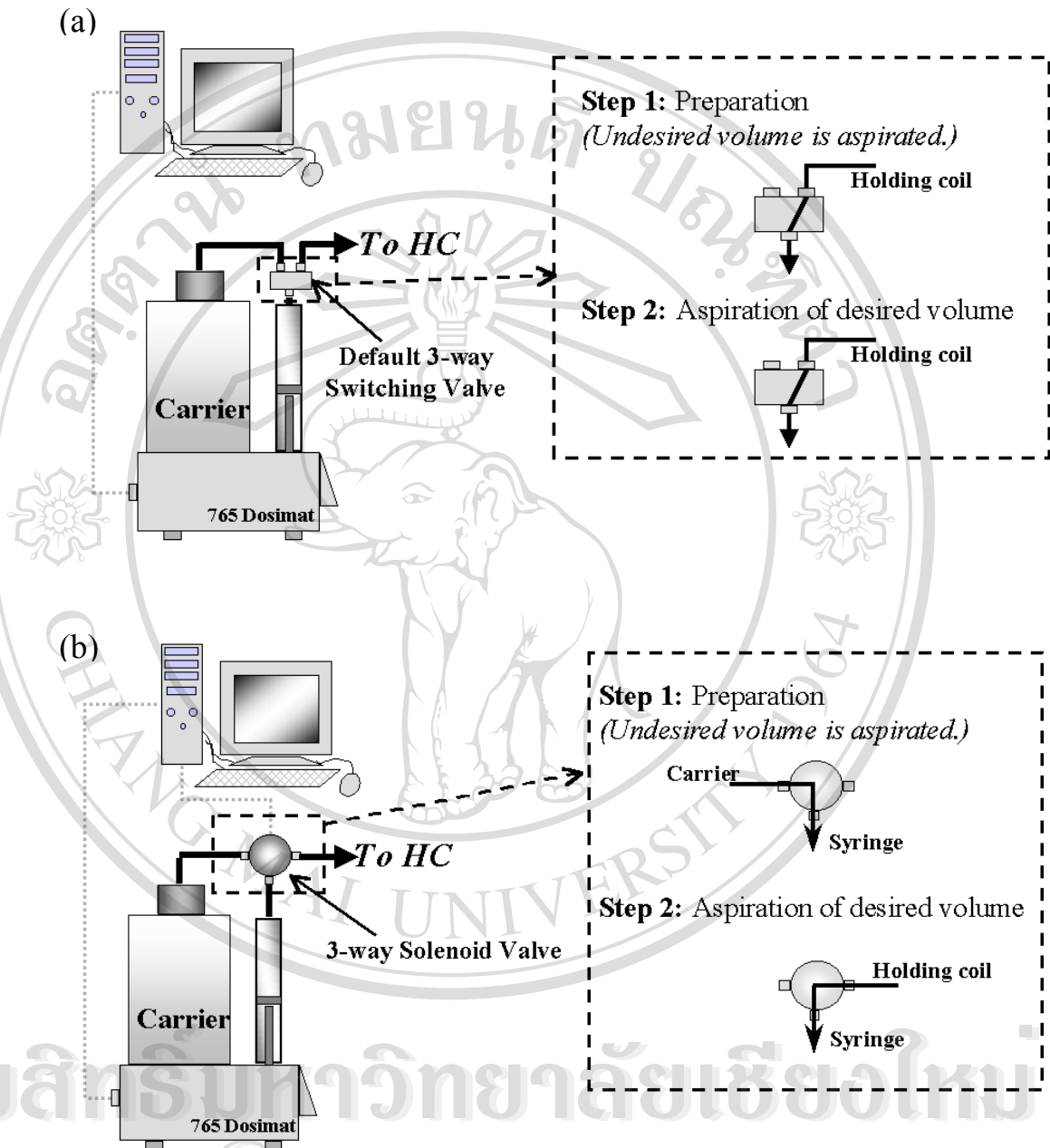


**Figure 3.21** (a) Working steps of the default 3-way switching valve of the autotitrator, (b) Working steps of the replaced 3-way solenoid valve

ลิขสิทธิ์มหาวิทยาลัยเชียงใหม่  
 Copyright © by Chiang Mai University  
 All rights reserved

### B) Sample Volume

Since the sample plug was propelled through the electrochemical flow-cell during the deposition step, the sample zone volume has to be correlated with the deposition time required to transport the sample zone through the cell volume. A deposition time of 45 s was applied in this study. Thus, the volume of the sample zone needed for this work is 0.375 ml, calculated from deposition time and flow rate (0.5 ml/min). The sequence of the SIA method is shown in **Table 3.6**, and the zones of aspirated solutions are illustrated in **Figure 3.22**.

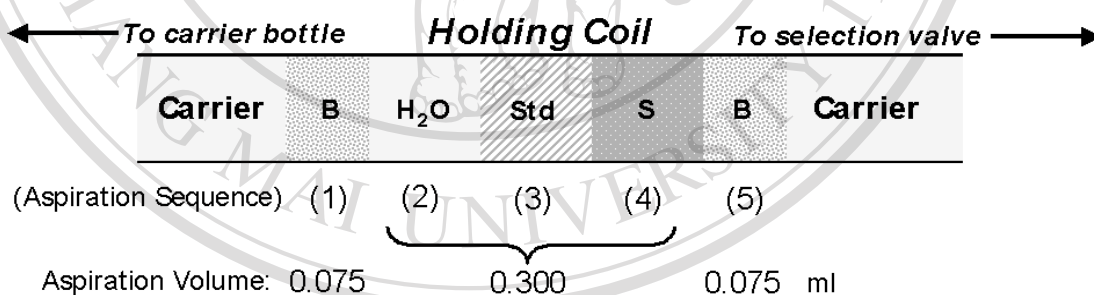


**Figure 3.22** Aspirated solution in holding coil; B: Buffer solution, Std: Mixed standard stock solution, S: Sample

### *C) Operation Sequence*

Operation sequences are shown in **Table 3.6**. The preplated MFE was prepared by the step 1 and 2. Acetate buffer solution, used as the electrolyte, was aspirated at the two ends of the sample zone (**Figure 3.22**) (step 3 and 7). The sample volume was fixed to 100  $\mu\text{l}$ . As on-line standard addition was made by the variation of the mixed standard stock solution volume, ultrapure water was included in the sample zone for the dilution of the standard solution. The performance of the developed SIA-ASV system *II* with on-line standard addition was tested. The voltammetric parameters were the same as those used with the FIA-ASV system (**Table 2.3**).

After the aspirated solutions were mixed by flow reversal in the holding coil, the 0.375 ml mixture zone was propelled through the electrochemical flow-cell for deposition of metal ions to the MFE, using the deposition potential of  $-0.8$  V. Then the flow was stopped for stripping the metal ions from the MFE by anodically scanning the potential of  $-0.9$  to  $0.15$  V. In the stripping step, the current signal is measured in the electrolyte medium. The 0.075 ml buffer solution was thus added at the end of the mixture zone. So the electrodes are in the electrolyte medium during the stripping step. After that, the excess solution in the flow cell was flushed out by step

**Table 3.6** SIA-ASV operation sequences

Step	Solution	Volume (ml)	Speed (ml/min)	Direction	Description
1	Hg(II) solution	5.100	5.0	HC	Aspirate Hg(II) to HC
2	Hg(II) solution	5.000	0.5	FC	Coating mercury film
3	Acetate buffer solution	0.075	1.0	HC	Aspirate buffer solution to HC
4	Ultrapure water	Varied	1.0	HC	Aspirate water to HC
5	Mixed standard solution	Varied	1.0	HC	Aspirate mixed standard solution to HC
6	Sample	0.100	1.0	HC	Aspirate sample to HC
7	Acetate buffer solution	0.075	1.0	HC	Aspirate buffer solution to HC
8	Ultrapure water	0.200	1.0	HC	Mix by flow reversal
9	Sample zone	0.365	0.50	FC	Dispense the sample zone to FC
10	Sample zone	0.375	0.50	FC	Deposit the metal ions on MFE
11	-	-	Stop	-	Strip metal ions and measure current
12	Ultrapure water	0.300	0.50	FC	Flush the solution in FC

#### ***D) On-line Standard Addition***

Different volumes of a mixed standard stock solution were added to the sample solution in order to perform standard addition on-line. The dispersion phenomenon in the tubing caused a dilution of the solutions in the holding coil (HC). However, the dilution factor in the HC was not known and had to be calculated. This was considered by recording a standard addition graph using a standard solution as a sample. Firstly, the standard addition graph was obtained by plotting the peak current against the standard volume (**Figure 3.23**). The intercept volume, ( $V_{std,g}$ ) calculated from the standard addition graph was then obtained. The metal standard concentrations ( $C_m$ ) were then calculated by,

$$C_m = \frac{C_{std} V_{std}}{V_{std,g}} \quad \text{Equation (3.1)}$$

where  $C_{std}$  is the metal concentration of the known-standard sample solution, and  $V_{std}$  is the volume of the stock standard solution. The calculated  $C_m$  was used further for plotting the standard addition graphs of metal in samples as illustrated in **Figure 3.24**.

The metal concentration in sample ( $C_s$ ) obtained from the standard addition of the sample is taken as the actual metal concentration in the sample.

It was very convenient to make on-line standard addition by the SIA system. A single mixed standard stock solution was used along the analysis. Only microliters of samples and standard solution were used in each measurement. Thus, the proposed on-line standard addition with SI system produced much less waste than the batch ASV method.

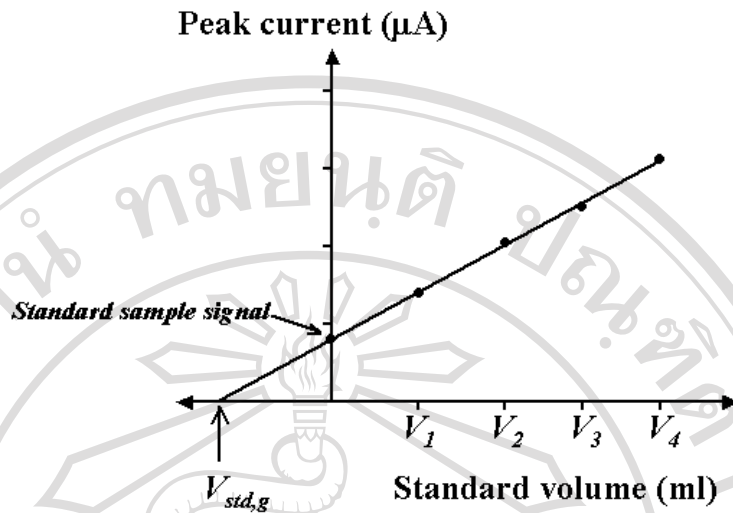


**Figure 3.23** Standard addition graph of a known-standard sample solution,  $V_1$ - $V_4$ : added stock standard volumes

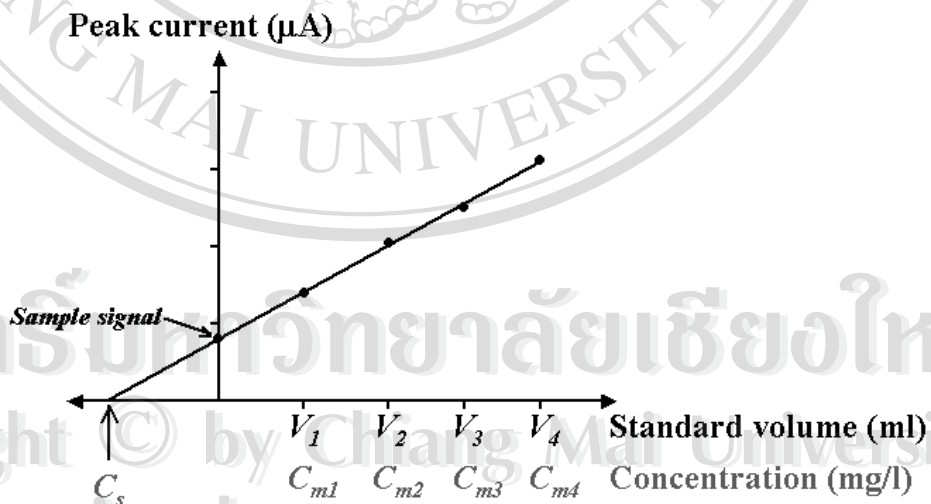


**Figure 3.24** Standard addition graph of a sample solution,  $V_1$ - $V_4$ : added stock standard volumes,  $C_{m1}$ - $C_{m4}$ : calculated concentrations of the added metal standard,  $C_s$ : metal concentration in the sample

### 3.3.3 Performance of the Developed SIA-ASV System II

Cd(II), Pb(II) and Cu(II) ions were determined simultaneously by the proposed SIA-ASV system. The voltammograms of the standard metal ions are illustrated in **Figure 3.25**. Peak potentials ( $E_p$ ) of Cd(II), Pb(II) and Cu(II) are  $-0.52 \pm 0.03$ ,  $-0.39 \pm 0.03$  and  $-0.05 \pm 0.03$  V, respectively. The peaks of the metals were resolved very well. The calibration data are summarized in **Table 3.7**. The proposed SIA-ASV system provided good linearity, low detection limits and low standard deviations. The proposed calculation method provided correct calculation of the metal concentrations. However, care has to be taken for the introduction of air bubbles into the system. Oxygen in air bubbles could be reduced at the MFE under the analysis condition (107) and thus decrease the sensitivity.

**Table 3.7** Calibration data obtained by the SIA-ASV system II

Metal ion	Dynamic range	Equation	R <sup>2</sup>	Detection limit*	%RSD (n=5)
Cd(II)	50-200 µg/l	$y = 8.523x + 0.132$	0.995	16 µg/l	2 % at 96 µg/l
Pb(II)	50-200 µg/l	$y = 7.480x + 0.336$	0.994	17 µg/l	2 % at 95 µg/l
Cu(II)	0.8-1.6 mg/l	$y = 4.399x + 1.182$	0.999	0.053 mg/l	3 % at 0.8 mg/l

\* defined as in (104)

All rights reserved

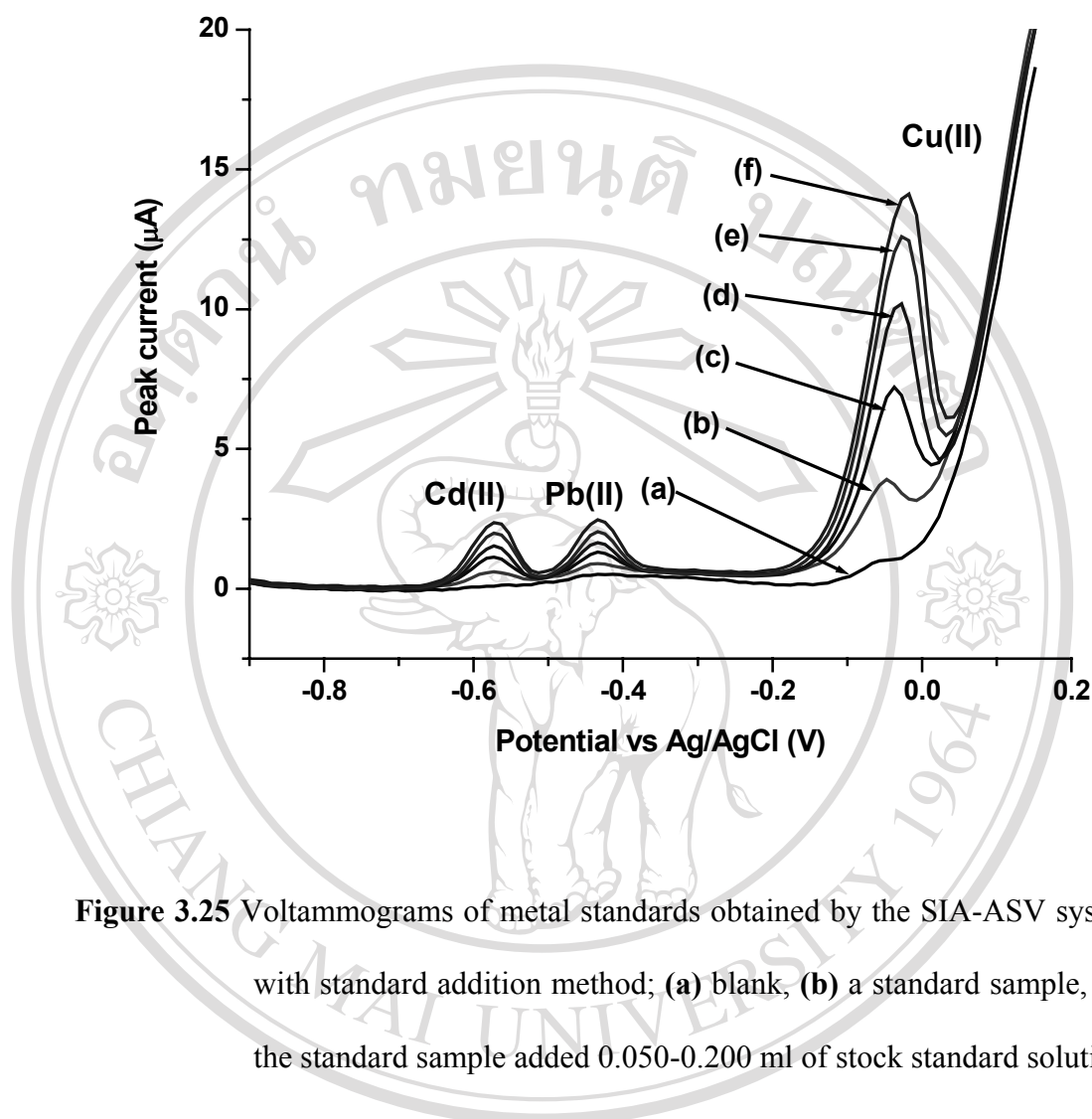


**Figure 3.25** Voltammograms of metal standards obtained by the SIA-ASV system II with standard addition method; (a) blank, (b) a standard sample, (c)-(f) the standard sample added 0.050-0.200 ml of stock standard solution

### 3.3.4 Application to Model Samples

The proposed SIA-ASV with on-line single standard addition was applied to two model samples (S1 and S2). The analysis results and the recovery percentages of Cd(II), Pb(II) and Cu(II) are shown in **Table 3.8**. The recoveries of the metals were satisfactory, except those of Pb(II). The reasons for the low recoveries found for Pb(II) have to be studied further. There might be some interferences in the sample.

However, further investigation of the developed SIA-ASV system should be made in order to verify the system, and to apply the SIA-ASV system for speciation of the dissolved forms of metals in the mixture solution, containing metals and organic colloids.

**Table 3.8** Analysis results and recoveries of Cd(II), Pb(II) and Cu(II) in the model samples obtained by the SIA-ASV system *II*

Sample	Concentration of Cd(II) (mg/l) ( $\pm$ SD)	% Recovery
S1	0.055 $\pm$ 0.001	89-108
S2	0.020 $\pm$ 0.001	98-106
Sample	Concentration of Pb(II) (mg/l) ( $\pm$ SD)	% Recovery
S1	0.074 $\pm$ 0.004	75-101
S2	0.036 $\pm$ 0.001	69-89
Sample	Concentration of Cu(II) (mg/l) ( $\pm$ SD)	% Recovery
S1	0.19 $\pm$ 0.01	94-105
S2	0.75 $\pm$ 0.03	99-119

### 3.4 Suggestions for Further Investigation

- 1) The commercial humic acid (Aldrich) used for leaching experiment and studying of colloid formation of the released metals was not purified. As the humic acid is extracted from soil and various extraction methods are used, there could be some elements present in the non-purified humic acid. Thus, the humic acid should be purified for the further study.
- 2) Because of the high dilution in the AF<sup>4</sup> technique, metal contents distributed with colloids in real water samples collected from the coal mining area could not be detected after the fractionation process. A sample preconcentration step may be needed for the analysis of colloid-borne metal ions in real water samples.
- 3) Since the developed SIA-ASV system is equipped with 2 PCs, one for controlling the SIA program and the other for controlling the ASV, the system is still not yet fully automated. The system has to be developed in order to attain a higher degree of automation by modifying the ASV program towards a higher compatibility with SIA.
- 4) The developed SIA-ASV system with on-line standard addition method provided satisfactory performance. However, the performance of the system should be further tested in order to allow the speciation of dissolved and colloidal metal ions in leachate samples and natural water samples containing natural organic matter.